GANAS

GAmma detection with New Advanced Scintillators

http://www.targisol.csic.es/ganas/

O. Tengblad, D. Cortina, I. Matea, M. Rousseau, R. Gernhäuser, C. Scheidenberger , A. Maj, P. Napiorkowski, D. Balabanski , D. Jenkins, F. Camera, C. Schmitt
GANAS CONSORTIUM

Nuclear physics is undergoing a renaissance with the advent of next generation radioactive beam facilities in Europe. These facilities will revolutionize our understanding of the atomic nucleus, particularly for exotic nuclei with extreme proton/neutron ratios. The knowledge obtained will also greatly improve our understanding of the formation of heavy elements in explosive astrophysical scenarios like supernovae.

Gamma-ray detection will continue to be a key tool for experimental nuclear physics. The new facilities make strong demands on the capability and performance of gamma-ray calorimeters. These challenges can best be addressed through the employment of novel scintillator materials such as lanthanum bromide. This led to a R&D programme where novel scintillator materials and advanced photosensors have been investigated. Further, we have explored new techniques and concepts such as phoswich detectors, segmented scintillators, and pulse shape analysis, and implemented this knowledge to applications.

Fig. 1 Distribution of the GANAS partners within Europe

Table 1. The GANAS Consortium

1 **IEM - CSIC**	Spain	IEM-CSIC, Serrano 113bis, ES-28006 **Madrid**	Olof Tengblad Olof.Tengblad@csic.es
2 **USC**	Spain	Facultad Fisica,Campus Vida s/n 15786 **Santiago de Compostela**	Dolores Cortina Gil D.cortina@usc.es
3 **IPNO**	France	15, rue Georges Clemenceau, 91406 **Orsay**	Iolanda Matea, Matea@ipno.in2p3.fr
4 **IPHC**	France	Institut Pluridisciplinaire Hubert Curien 23 rue du Loess, BP 28, 67037 **Strasbourg**	Marc Rousseau Marc.rousseau@iphc.cnrs.fr
5 **TUM**	Germany	Technische Universität München Physik-Department E12 James-Franck-Straße 1, D-85748 **Garching**	Roman Gernhäuser Roman.Gernhaeuser@ph.tum.de
6 **U. Giessen**	Germany	Physikalisches Institut, Heinrich-Buff-Ring 16, 35392 **Giessen**	Christoph Scheidenberger Christoph.Scheidenberge@exp2.physik.uni- giessen.de
7 **IFJ PAN**	Poland	Inst. of Nuclear Physics Polish Academy of Sciences, Radzikowskiego, 31-342 **Kraków**	Adam Maj Adam.Maj@ifj.edu.pl
8 **ŚLCJ**	Poland	Heavy Ion Laboratory, University of Warsaw, Pasteura 5a, 02-093 **Warsaw**	Pawel Napiorkowski pjn@slcj.uw.edu.pl
9 **INRNE**	Bulgaria	Institute for Nuclear Res. and Energy Bulgarian Academy of Sciences, 72 Tsarigradsko Chaussee Blvd. 1784 **Sofia**	Dimiter Balabanski Balabanski@inrne.bas.bg
10 **U. York**	UK	Department of Physics, University of York, **York** YO10 5DD	David Jenkins david.jenkins@york.ac.uk
11 **INFN - U. Milano**	Italy	Univ. of Milano, Department of Physics, Via Celoria 16, 20133 **Milano**	Franco Camera franco.camera@mi.infn.it
12 **GANIL**	France	Bd Henri Becquerel, BP 55027, 14076 **Caen**	Christelle Schmitt schmitt@ganil.fr

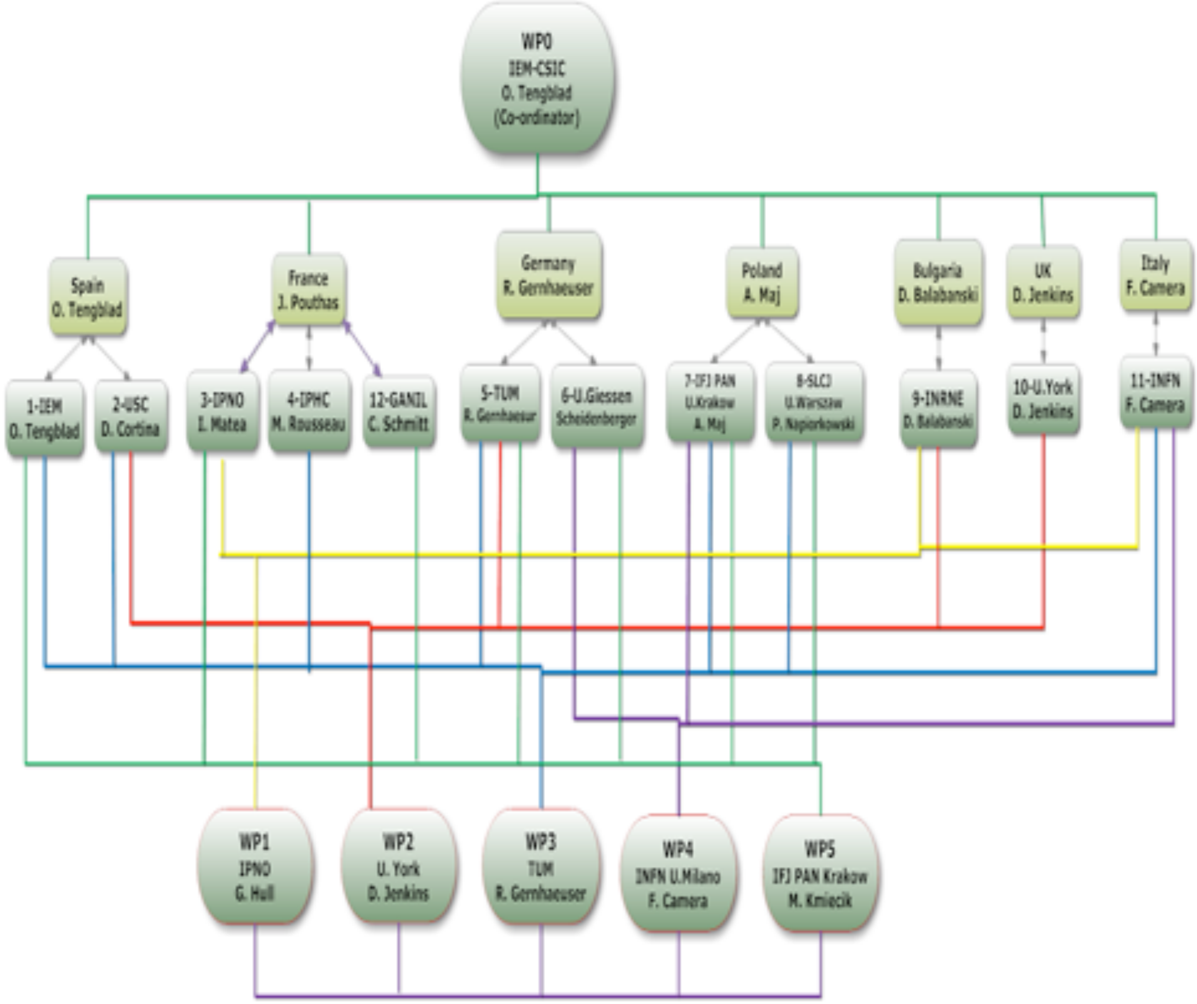

Fig. 2 The Organigram of the GANAS consortium

BACKGROUND

During the past decade it has been demonstrated that reactions with exotic secondary beams are an important tool for exploring the properties of nuclei far from stability, and allow detailed spectroscopic information to be extracted. The physics motivation for studying reactions with exotic nuclei is described extensively in various reports in the context of next-generation facilities, e.g. the future FAIR project at GSI http://www.fair-center.eu/ or the SPIRAL2 project at GANIL http://pro.ganil-spiral2.eu/spiral2/what-is-spiral2/physics-case/view. In addition, fusion-evaporation reactions induced by high intensity neutron-rich beams from SPIRAL2 will make it possible to populate exotic compound nuclei at a much higher initial angular momentum than currently achievable with stable beams. This will be of strong benefit in the study of vibrational and rotational collective phenomena at high spins and finite temperature, such as the Giant Dipole Resonance or exotic shape changes induced by fast rotation. Heavy-ion radiative capture and reaction dynamics studies will also benefit considerably from the availability of high-intensity neutron-rich beams.

As gamma-ray detection constitutes an important experimental probe common to all these physics topics, the powerful future accelerator facilities require a new generation of gamma detector arrays capable of exploiting the full potential of these highly exotic or high intensity beams. Very recently, new technologies, materials and techniques have been developed and large international collaborations have been formed for the development and construction of large detector arrays like CALIFA (R^3B) at FAIR or PARIS at SPIRAL2.

The R^3B set-up at FAIR will concentrate on experimental reaction studies with exotic nuclei far from stability, with particular emphasis on nuclear structure and dynamics and reactions of astrophysical interest. The R^3B programme will focus on the most exotic short-lived nuclei, which cannot be stored and cooled efficiently, and on reactions with large-momentum transfer allowing the use of thick targets. The proposed experimental setup is adapted to the highest beam energies delivered by the Super-FRS, thus making full use of the highest possible transmission efficiency of secondary beams. A crucial part of the R3B set-up is the gamma-ray spectrometer CALIFA that surrounds the reaction target. This spectrometer is designed to detect gamma rays up to 30 MeV and protons up to 700 MeV, with high angular resolution to permit a full kinematic reconstruction. Due to the relativistic energies involved, the gamma rays are strongly Doppler shifted, which is why a very high segmentation of the detector is needed in order to be able to make the right corrections to he obtained data.

The main aim of the PARIS collaboration is to develop and construct a dedicated gamma-calorimeter with dynamical range from 100 keV to 50 MeV. PARIS is designed to be used primarily at SPIRAL2 but could be portable and be used at other facilities such as FAIR or HIE-ISOLDE. At SPIRAL2, PARIS will be used in conjunction with other detectors such as AGATA, NEDA, and GASPARD. PARIS therefore needs to be a highly modular and versatile device.

In-beam and decay studies of the rarest isotopes produced at next generation radioactive beam facilities will shed light on the structure of nuclei approaching the drip-lines. This is central to a deeper understanding of the isospin dependence of nuclear forces, and our understanding of different nucleosynthesis processes in our Universe. Gamma-ray detection constitutes an important experimental probe common to all these physics topics. High-resolution gamma-ray spectroscopy is still one of the most important tools in nuclear physics. The unique opportunities of the next generation RIB facilities bring with them strong experimental challenges and the obligation to make best use of the high investment in delivering RIBs. The optimum gamma spectrometer will therefore combine a maximum of solid angle with good rate capability and energy resolution. New scintillator materials and photon detector technologies in combination with high granularity will push forward the experimental limits of Doppler shift at relativistic energies at a quite reasonable amount of investment. Detector setups need to be versatile to satisfy the demands of a wide range of different experiments ranging from the detection of low energy gamma rays from single particle excitations, high energy gamma rays associated with different collective modes, up to the detection of charged particles emitted from the reaction zones. In the case of quasi-free scattering reactions, low-energy gamma rays have to be detected with high resolution in coincidence with protons of up to 700 MeV. On the other hand, in Coulomb-excitation experiments, it is necessary to fully absorb high energy gamma rays from collective modes that are Doppler shifted by up to a factor of three. When using relativistic energy beams, it is also very helpful to have a good neutron-gamma separation to suppress background as well as a $\Delta E/E$ measurement to identify charged particles without additional assumptions on the reaction. Decay experiments dealing with extremely low production yields of the nuclei of interest, and suffering from enormous radiation from strong competing channels as well as from the environment, requires excellent background suppression capability.

INTRODUCTION TO THE PROJECT

In the ERA-Net NuPNET 1st call for transnational joint activities, a strong collaboration for the future developments in the field of scintillation detectors was formed. The consortium with the label GANAS started to work in 2012 straight after the application was granted with highest rank. Within the project large sets of experimental data have been generated at different sites. New algorithms have been tested already online and optimized for selectivity and efficiency. The analysis of these data-sets allowed for the development of new powerful and fast algorithms that could be implemented in FPGA based hardware typically used in modern experiments.

The objective of GANAS was to make R&D on new scintillator materials and sensors in order to make implementation of these innovative technologies for the construction of Nuclear Physics Detectors, especially for the detection of gamma and high energy charged particles.

This research program addresses the development of technology in relation to scintillator detectors. In WP1 different novel materials have been identified and studied. WP2 has dealt with different kinds of readout sensors. In WP3 Pulse shape analysis has been adapted to improve and optimize the detection efficiency and identification between different type of radiation and of different dynamic energy ranges. WP4 has specialized the R&D on the need to localize the interaction points of gamma-rays inside a large volume scintillator crystal and to set the basis for the construction of a position sensitive large volume scintillator detector for γ-rays of medium-high energy has been. Finally, the WP5 has studied the combination of different scintillator materials in the same detector to obtain specific segmentation of crystal and thus gain new detection information. Further, simulation, production and test of prototypes, which are capable to provide, on an event by event basis, the image produced by the scintillation light on the photocathode, have been performed.

Position sensitive gamma detectors are employed for a wide range of applications from physics research, bio-medicine to applications in the civil sector like oil investigations. Determining the first interaction position of a gamma ray in a detector is important for high-resolution in-beam nuclear spectroscopy experiments to be able to correct the Doppler Broadening of the gamma lines. This broadening occurs when the gamma ray source moves with high velocity and is caused by the angle dependent Doppler shift over the opening angle of the detector. The localization of the interaction point of the gamma ray inside the crystal and the tracking of the gamma ray while it is undergoing multiple scattering allows the correction for this effect.

The GANAS project has led to significant advances in exploring the coupling of solid state devices such as silicon photomultipliers to scintillator crystals. Over and above this, however, it has brought the groups into close engagement with industry. In collaboration with Kromek PLC, the UoY group developed a commercial product; a hand-held gamma-ray spectrometer. A variant of this is now achieving considerable commercial success. The success of this initial work within GANAS has led to further work funded by UK funding bodies, direct industrial funding and the US Defence Threat Reduction Agency.

At the beginning of the GANAS project almost nothing was known on the imaging properties of position sensitive detectors that use several centimetres thick scintillator crystals and measure medium-high energy γ-rays. The GANAS project has stimulated a coordinated effort to start the R&D activity necessary to successfully tackle this topic. The project has, in addition, produced several published works and conference communications which would not have been possible without the GANAS project.

It is also important to stress the synergy and the collaboration works between the different component of the GANAS collaboration.

These developments in detector technology for nuclear physics such as the novel scintillators together with novel sensors have considerable relevance also to societal applications outside fundamental research. Such applications span a broad range from medical imaging to homeland security and oil and gas exploration.

The GANAS project was organized into different work-packages (WPx):

WP0 Management:

As international co-ordinator of the project, IEM-CSIC has hosted the project website http://www.targisol.csic.es/ganas/ and kept it up to date. In 2013 was organized two weeks of test experiments at the proton cyclotron in Krakow where all GANAS groups, each with its various scintillators and different sensors as well as using different data collection systems, were involved. We have also held several meetings of the GANAS-consortium to discuss progress and the possible continuation of collaboration over the time of the project.

The GANAS project has performed well, all participants have advanced in their tasks and met the objectives. WP5 and especially the participants IFJ Pan Krakow and INFN Milano were delayed by production problems; scintillators LaBr / NaI for PARIS detector and therefore the project had two extensions approved by the ministries of the different countries finally the GANAS project finished officially the 30 of December 2015. This document concise the final report of the project bringing together the contributions of the different groups.

The collaboration prepared in 2013-14 the continuation of the activity within the Horizon2020. The new proposal was presented by O. Tengblad to the conference of ENSAR http://www.ensarfp7.eu/what-is-ensar/workshops-schools/ensar-town-meeting. The result has been the continuation of GANAS as the Joint Research Action PASPAG within the international ENSAR2 project that was approved by the European Union with a start date of 1st of March 2016, see http://www.ensarfp7.eu/ (page provisional).

WP1 New Scintillators Materials:

The main objectives of this work package (WP1) was the characterization of new advanced scintillator materials and to assess the performances for its use in a gamma spectrometer obtaining the properties requested for the PARIS and CALIFA detectors.

The ideal inorganic scintillator should provide not only a high light yield but also a high effective atomic number for good stopping power, a short decay time constant for fast response, and a good level of linear response for good energy resolution. In addition, chemical and mechanical robustness are needed to allow the scintillator detector to be used in many different applications and environments. The Fig. 3 display a schematic ordering of the existing materials as a function of the expected energy resolution that can be obtained with them.

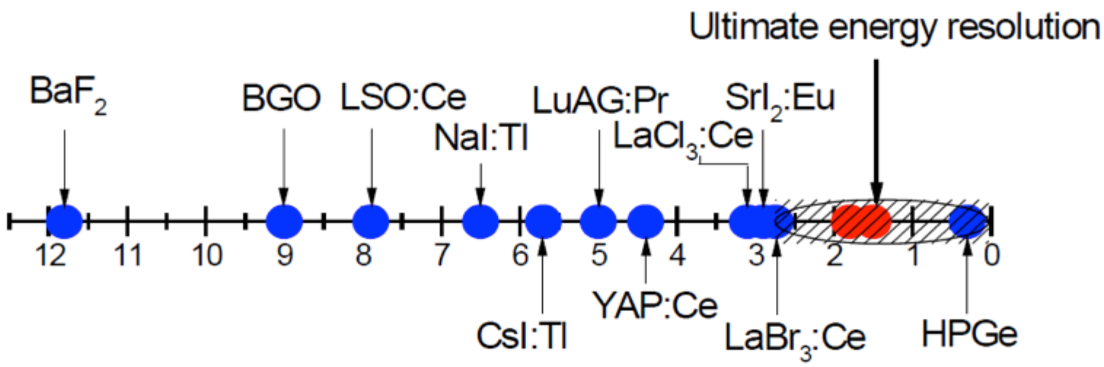

Fig 3. Existing High resolution scintillator materials ordered according to the energy resolution that can be obtained: FWHM of ΔE/E in % at 662 KeV.

Over the latest years there is a renewed interest, in the chemistry and material science community, to search for new luminescent inorganic crystals as real alternatives to NaI and CsI crystals that have energy resolution only in the order of 6-8% and instead obtain materials like $LaBr_3$:Ce with a resolution < 3%. While many of the new proposed scintillators are still in the developing process and are not available in sizes suitable for our interest, there are few, as $CeBr_3$ or SrI_2:Eu, that have already been grown in cm^3 scale samples. In particular, $CeBr_3$ provides a light yield of 68 photons/keV and a fast decay time and SrI_2:Eu, while being brighter with a light yield close to 100 photon/keV, has a long decay time constant (around 1 μs) and a very linear response.

A field of interest for the proposed study has concerned scintillating transparent ceramics. This means the study of different solution for the proper encapsulation and packaging of the crystals as well as in the optical coupling with the most suited photo detector. The encapsulation gives an external pressure to the crystal that seriously affects the optical response and can be connected to the non-proportionality that many scintillator materials exhibit. Further, the crystals structure, dopant concentration, concentration in caption substituted materials and crystals structure also can be related to the light output and non-proportionality of the response, especially at very low energies see Fig. 4.

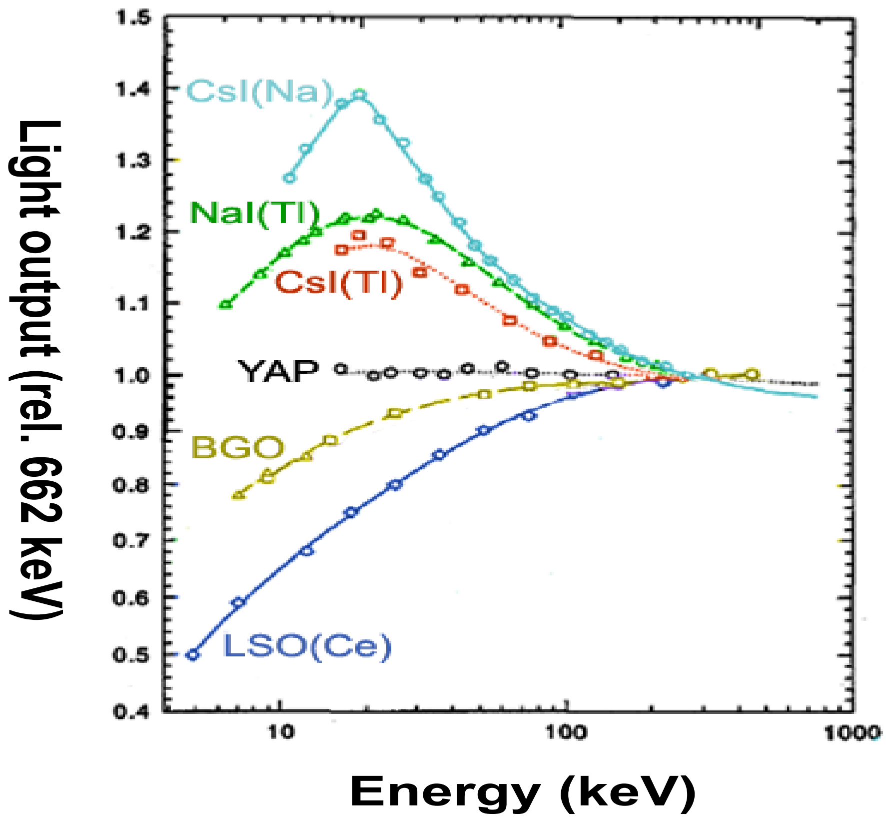

Fig 4. Light output vs Energy for some typical scintillators.

Especially, the detection properties of new advanced scintillator materials like $CeBr_3$ and SrI_2 are tested for their use in a gamma spectrometry. Also different Phoswich combinations like: $LaBr_3$-CsI, LaBr-LaCl, LaBr-NaI have been studied. Furthermore, a network with expert laboratories and companies that produces these new promising scintillator materials was created. IPNO received for the GANAS project 39 k€ over the first two years. This money was used to procure new advanced scintillator crystals and photomultipliers tubes for testing, see Table 2.

Table 2. Procured and tested scintillator materials and PMTs at IPNO & INFN.

Crystal	Geometry	Manufacture	Price	Delivered
CeBr3	Ø 25 mm x 25 mm	Scionix	1.475 €	I 2011
CeBr3	Ø 51 mm x 76 mm	Scionix	15.200 €	2012
SrI2:Eu	Ø 25 mm x 25 mm	RMD	9.420 €	2013
CLYC	Ø 25 mm x 25 mm	RMD	5.701€	2013
CLYC	1”x1”	RMD		2012
LaBr3	1”x1” - 3.5” x 8”.	Saint Gobain		2010-2013

PMT	Features	Manufacture	Price	Delivered
5 R7723-100	Ø 51 mm – SBA photocathode 8 dynodes	Hamamatsu	478.80€	2013

Scintillator characterizations: The five scintillators procured within the frame of the GANAS collaboration were tested in May 2013 during an in beam testing of clusters for the PARIS demonstrator. This campaign led us to test the scintillators at gamma ray energies not available with standard radioactive sources. Each scintillator was coupled to a R7723-100 photomultiplier tube from Hamamatsu, as used for the phoswich light readout by the PARIS collaboration, and the signals were collected by a 1 GS digitizer for offline analysis. This work was published in [1] and [2] see the publication list at the end.

At IPNO the CeBr3 crystals have been fully characterized with gamma ray emitting sources in the energy range between 60 to 1408 keV. In particular, was measured the light yield, the energy resolution, the gamma ray proportionality and, for the 76 mm thick CeBr3, the light yield uniformity [3].

The tests have been performed coupling the crystals to a PMT Hamamatsu R7723-100, equipped with a Ø 51 mm entrance window and a super-bialkali photocathode. The gamma ray spectra have been acquired with a standard spectroscopic chain: the anode signal from the phototube was sent to a Cremat 113 preamplifier, then shaped with an ORTEC spectroscopy amplifier and finally collected with an ADC. For the two CeBr3 crystals we measured an energy resolution at 662 keV of 4.8% and 4.7% for the small and the big volume crystal respectively [4].

At INFN in Milano the large volume LaBr3:Ce detectors have been fully characterized. The detectors were tested using monochromatic gamma-ray sources and in-beam reactions producing gamma-rays up to 22.6 MeV. PMT signal pulses were acquired and the detector energy resolution and linearity of response as a function of gamma-ray energy was extracted. Two different voltage dividers were coupled to the PMT: the Hamamatsu E1198-26, based on straightforward resistive network design and the “LABRVD”, specifically designed for our large volume LaBr3:Ce scintillation detectors, which also includes active semiconductor devices [5] We also estimated the time resolution of different sized detectors (from 1”x1” up to 3.5”x8”), correlating the results with the intrinsic properties of PMTs and the GEANT simulations of the scintillation light collection process.

Concerning the measurements with the 1”x1” CLYC scintillator in Milano, the measurements are still in progress. We plan to compare the scintillator response using different PMTs, voltage dividers, and values of HV. We will measure energy resolution with different shaping times, preamplifiers and for different gamma rays energies. In addition, we will continue these studies by also measuring the neutron response using PSA digital technique and the specific modules we have designed for BaF2 and LaBr3:Ce.

WP2: photo sensors:

The work-package WP2 was concerned with research and development on novel sensors for optimizing the light collection of the new scintillator materials. This has potential application to detectors used for charged particle, neutron and especially, gamma ray detection in nuclear physics experiments. The devices of interest are large-area avalanche photodiodes (APDs) and silicon photomultipliers (SiPMs). APDs are silicon-based photosensors which convert light to an electrical signal. Typically, APDs achieve a first-stage gain of around 100. SiPMs are small, highly dense arrays of APDs which can provide high gain ($>10^5$) comparable to that of a standard photomultiplier tube (PMT) and will become a generic replacement in the future if they can compete in terms of costs and performance. Both APDs and SiPMs have the strong advantage compared to PMTs that they can be operated in regions of high magnetic field, which are often present around or inside large electromagnetic elements used in nuclear physics experiments. They also have a potential role in societally important applications such as simultaneous PET/MRI imaging.

LAPDs:

Large area silicon avalanche photodiodes (APD) when used with different scintillators can be an excellent soft gamma-ray detector. In particular, so called reverse type APD is well suited for these applications due to very narrow, no more than 8 μm thick, high gain layer close to the light entry surface and optimized for high efficiency detection of short wavelength radiation. The special gain profile provides amplification where it is needed and does not introduce additional noise in the rest of the structure, which has a wide depletion region necessary to minimize device capacitance. Low device capacitance is important parameter from the point of low noise operation requirements when connected to interface electronics, but in this case is aggravated by device very large size and only through this special design it has been possible to achieve acceptable capacitance while keeping breakdown at reasonably low level at the same time.

Currently there is mainly one producer (HAMAMATSU) on the market that provides a detector series fulfilling all the requirements for devices large enough to be used in large volume scintillation detectors. The Hamamatsu series S8664 has a typical leakage current of 10 nA at gain of 50 and a terminal capacitance of 270pF in the case of the largest devices of 100 mm^2. There is some development going on to change the shape of this device e.g. for the panda experiment, but currently not too much effort is put into this development of large-size sensors. Our recent investigations have shown that increasing the active area from 1 cm^2 to 2 cm^2 in order to adapt the size of the sensor to the output-surface of the scintillator, significantly improves the performance of the scintillation detector.

The USC team has specialized in the use of these Large Area Avalanche Photo Detectors, LAAPDs, as light sensors for large CsI (Tl) scintillator. This was a joint development with the producer (HAMAMATSU) to increase the surface of these sensors which resulted in the development of a specific ceramic mask that houses two of the photo-sensors powered by a single input voltage. To assess the quality and performance; a protocol of measurements and quality control of the LAAPD including gain-calibration (amplitude) vs applied voltage, and the influence of the applied voltage to the final energy resolution, was established. The work has allowed to optimize the LAAPDs that are to be used as sensors for the detection units of CALIFA. Especially the work has been related to select and group together the LAAPDs according to optimized supply voltage and leakage current. For the realization of this work a specific test bench was developed that has allowed to determine the critical parameters for optimal performance of the photo sensors, based on the comparative study of more than 400 units.

At the same time work on optimizing the quality of crystals of CsI (Tl) which should couple to these APDs have been done. These scintillator crystals are very large (up to 22 cm long) and to obtain optimum resolution it is important that the concentration of the dopant is maintained constant along the crystal in order to to minimize possible inhomogeneity's in the light-collection (LONU). A degradation of LONU translates into different light-output depending on the point of interaction and thus a direct impact on the energy resolution of the device. In addition to a strict specification in terms of uniformity in the concentration of dopant, the crystals of CsI (Tl) selected for this work are following a process of local polishing (lapping) that reduces the LONU to acceptable levels. [6],[7].

Once all the comparative studies of individual elements have been performed, the photo sensors are attached to the scintillator crystals and prototype-detectors of different size have been constructed. Testing has been performed with these prototypes of its behaviour to gamma radiation in the local lab and at different international laboratories. This last activity was performed in an international context where the group of USC worked in close collaboration with the groups of IEM-CSIC, TUM (Germany) and IFPJ - Krakow (Poland). The experiments have been performed at the Tandem laboratory of TUM (Germany), at GSI (Germany) and at the proton cyclotron in CCB - IFJ-PAN (Poland).

SiPMs:

SiPMs are good candidates for the read-out of detectors due to their small size, high sensitivity to single photons, efficiency, insensitivity to magnetic fields, low bias voltage, fast timing and linear pulse height response. These properties bring SiPMs in the discussion to be used for gamma spectroscopy with scintillator detectors. Here the use of SiPMs is considered in the context of achieving good energy resolution. In the performed research, different size and type of SiPMs were tested coupled with different kinds of scintillation materials and results are compared with results obtained with regular Photo Multiplier Tubes.

Principle of the Counting Process by Using SiPMs: SiPMs consist of arrangements of a large number of photodiodes working in Geiger mode, operated at reverse bias. When an incoming visible light scintillation photon interacts in the depletion region around the p-n junction, it could excite an electron to the conduction band, creating an electron-hole pair. When an electric field stronger than about $5x10^5$ V/cm is applied, the charge carriers have enough energy to create secondary charge pairs and to initiate an ionization cascade in the silicon volume. The diode breaks down and becomes conductive. This process is called Geiger discharge. The respective electron avalanche is quenched, developing a voltage drop on a series resistor. A diode-resistor pair is called micro-cell. The sum of the fired micro-cells of a SiPM coupled to a scintillator is proportional to the initial energy deposited.

Survey of available sensors:

Further, within this work package, APDs have been evaluated in conjunction with the LaBr3 scintillators. Energy resolutions of 6-7 % and timing resolutions of 1-2 ns were measured. APDs can be used for nuclear physics studies and wider applications in medical imaging and elsewhere. The insensitivity of the prototype systems to magnetic field has been verified.

The principal manufacturer of APDs is Hamamatsu. Although we used mostly Hamamatsu APDs and SIPMs, it is worth mentioning that there are few other companies which make SiPM-sensors including SensL (Ireland) and Photonique SA (now available from Advatech-UK). Photonique's sensors originate from CPTA Russia. These were not particularly useful to us as their efficiency in lower wavelength (380 nm i.e. $LaBr_3$:Ce) was negligible. Some measurements were also made using SiPMs from Hamamatsu – models 10362-11-025U and 10363-33-025C which were 1mm x 1mm and 3mm x 3mm in size. The 1 mm device was not useful for making an energy measurement due to its small size and thus small light collection efficiency, but it was possible for it to be used as trigger for timing. We also tested some of SensL's earlier devices like their 4 x 4 array (or tile) but their efficiency was again not anywhere close to being suitable for use with $LaBr_3$(Ce). These devices may, however, be used in imaging applications where the scintillation photons are longer wavelength (500-600 nm). We have future plans to build a small imaging system using 4 x 4 two dimensional arrays where we plan to do a comparison between the Hamamatsu and SensL device (4 x 4 tile) which are both sensitive to the higher wavelength region where emission takes place in LYSO and BGO. TUM, the *Technische Universität München,* started in collaboration with Laser Components Inc. a new development to produce fully functional 10 x 20 mm active area LAAPDs, which shape and size is not commercially available at the moment. This project co-funded by the BMBF was focused on prototypes mounted on a ceramic subcarrier with device completely immersed in clear plastic coating.
These sensors were directly compared to the Hamamatsu sensors in order to specify essential parameters for spectroscopic light detection; temperature dependence, spectral response, signal rise time, gain curves stability, and radiation hardness. Having more than one producer on the market would strongly influence further developments as well as the price policy.

Towards applications:

Scintillation detectors are important for charged-particle and gamma-ray detection both in nuclear physics, and medical and industrial applications. Conventionally, the best performance in terms of scintillation light collection is obtained with photomultiplier tubes (PMTs). Such PMTs cannot be operated in regions of high magnetic field. This imposes a strong restriction on the efficient employment of scintillator detectors in high magnetic field environments commonly found in various apparatus of interest in nuclear physics. In addition, there is very strong interest in the medical sector in combined imaging where it is desirable to perform positron-emission tomography (PET) or single-photon emission computed tomography (SPECT), which provide functional information, simultaneously with MRI, which provides anatomical information. This means that the scintillator-based technologies associated with PET or SPECT would need to be operated within the high magnetic field of an MRI magnet. It turns out that this need from the medical side aligns very well with topical interests in nuclear physics, where gamma ray detection is required in high magnetic field environments. Imaging systems, however, have two additional constraints. One is that RF-induced noise may affect the performance of the PET system. The second is the magnetic field is more susceptible to the placement of external objects (i.e. sensors and detectors).

A prototype gamma-ray detector system which could be used in high magnetic field environments has been evaluated. A specific project of interest is a gamma-ray detector array to be used in conjunction with a helical-orbit spectrometer such as the HELIOS spectrometer at Argonne National Laboratory. Such a spectrometer is intended to study single-particle transfer reactions in inverse kinematics. The spectrometer comprises a large solenoidal magnet (such as a redundant MRI magnet) in which light ions from the reaction follow helical orbits before being detected along the axis in a compact linear silicon array. Detection of gamma rays would assist in assigning j values to observed states and in other applications. In this case, the gamma ray array would need to have high energy resolution but be capable of operating in a magnetic field up to 3T. With the intention of achieving the highest possible energy resolution we considered the new generation scintillator material, lanthanum bromide ($LaBr_3(Ce)$), which has an intrinsic resolution better than 3% for 662-keV gamma rays. For the scintillation light collection, we focused mainly on APDS since they have low noise and good temperature stability. However, SiPMs (which are arrays of APDs working in Geiger mode) were also studied for the sake of completeness.

Prototyping: The simple prototype which was the main goal of the study was constructed from a Hamamatsu APD with an LaBr3(Ce) scintillator. The APDs used were S8664-1010 and S8664-55 devices that had dimensions of 10mm x 10mm and 5mm x 5mm, respectively. The LaBr3(Ce) crystals are from St Gobain and are in a cylinder of 1cm diameter and 1 cm depth encased in an aluminium canister. The APDs were mounted on a small PCB with a non-magnetic SMC connector on the back. Since the scintillator face was 10 mm, which was close to the sensor dimensions, no light guides were used. The mounting of the APD on the scintillator was done using EJ-550 silicone gel obtained from ELJEN technologies and the sensor/detector system was wrapped in several layers of Teflon tape. Finally, they were wrapped in Al foil and then black masking tape to make them light-tight. The whole assembly was less than 15 cm^3 and connected to the preamplifier by a single cable. The Mesytec unit MSI-8p was used as the preamplifier along with an Ortec 572 shaping amplifier for shaping and amplification. Power to the sensors was provided using Mesytec MHV4 unit. Figures 5 and 6 show the performance of the sensor/scintillator system using ^{60}Co and ^{137}Cs sources, respectively.

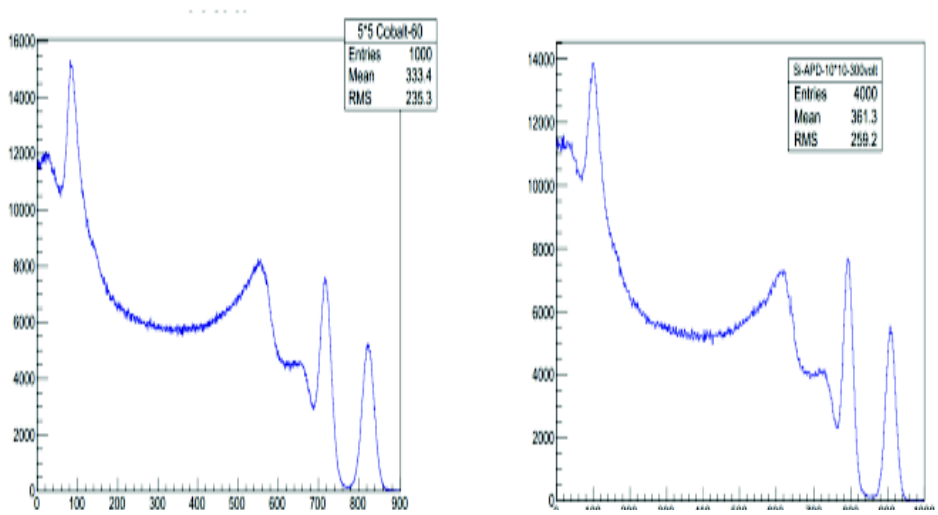

Figure 5. ^{60}Co spectra using a 5 x 5 mm and a 10 x 10 mm APD with $LaBr_3(Ce)$ scintillator with energy resolution of 4.23 % and 3.57 % at 1332-keV

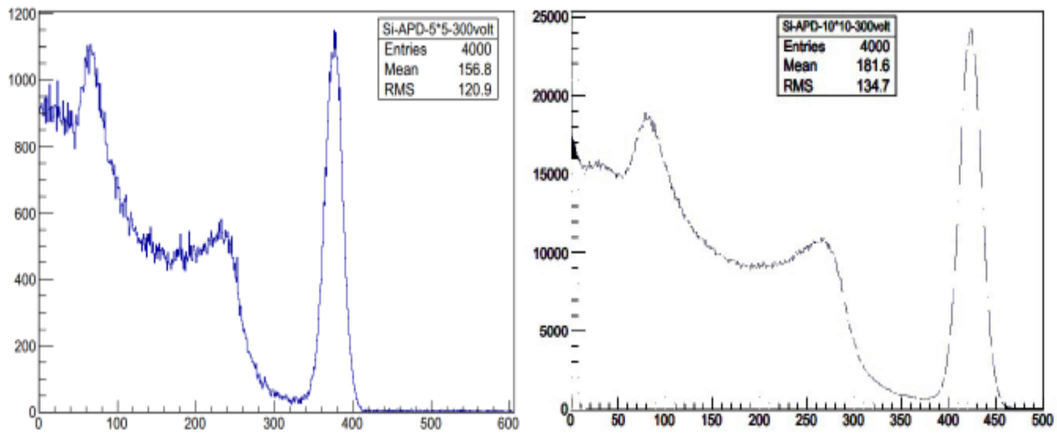

Figure 6. [137]Cs spectra using 5 x 5 mm and 10 x 10 mm APD with $LaBr_3(Ce)$ scintillator with energy resolutions of 7.3 % and 6.7 %, respectively, at 662 keV

Magnetic field measurements: The performance of the prototype systems in a magnetic field was evaluated using a 1T magnet available in the Department of Physics at the University of York. The magnet belongs to the magnetic materials group and is a simple DC current magnet with sufficient in-pole gap to place the detector and APD. The preamplifier and the counting system remained on a trolley nearby. A ^{137}Cs source was used for the experiment and the measurements were done in the same setting with and without the 1-T magnetic field. The effect of the magnetic field on the performance of the detection system was found to be negligible. These measurements were then repeated by changing the orientation of the detector with respect to the magnetic field placing the detector axis perpendicular as well as parallel to the field axis. None of these measurements showed any deterioration in the performance in the magnetic field therefore suggesting that such a device would not be affected by the magnetic fields typically found in MRI magnets.

Although APDs were the main focus of the tests, it was found that SiPMs showed similar insensitivity to magnetic field, which is not so surprising given they are 2D array of tiny APDs and therefore, supposed to have similar characteristics. There was still the question of whether the insertion of the sensor and scintillator would modify the magnetic field or not. In order to investigate this aspect, we decided to perform an MRI scan of a phantom with the detector unit placed next to the phantom. The scan was performed at the York Neuroimaging Centre (YNIC). Due to a restriction imposed by YNIC, it was not possible to place measuring instruments (NIM bin, preamp etc.) inside the room containing the MRI machine. It was also not possible to use radiation sources within the facility. However, it was still possible to place the detector and the cables unit within the magnet's centre alongside a phantom (a plastic ball filled with paramagnetic substance + H_2O) and perform a scan to see if any distortion to the image occurs. We used a 10 x 10 mm APD mounted on a 2.5 cm x 2.5 cm CsI(Tl) crystal and 5 x 5 mm APD mounted to an $LaBr_3(Ce)$ encapsulated in aluminium. The connectors had 5 m long RG58 shielded cables connected with them. The images acquired by scanning this system showed that the there was a small influence on the magnetic-field homogeneity from the detector set-up when it was placed alongside the phantom which was placed close to the axis of the magnet. The distortion caused to the image was small and it was possible to correct it using the shimming coils available in the MRI system. Placing the detection set-up far away from the axis, where most likely it would be used in a research set-up like HELIOS or in an imaging scanner (PET insert for an MRI scanner), did not show any image distortion of the scanned object.

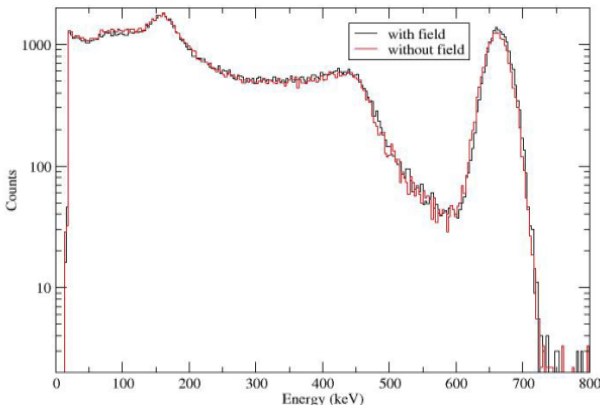

Figure 7. A representative set of spectra for a 137Cs source obtained with and without 1T magnetic fields. The 3T MRI magnet at the York Neuroimaging Centre. The detectors are placed on the side of circular cage shown in the centre of the magnet. The cables from the detectors can be seen stretching along the bed.

Timing measurements: Timing measurements were also performed using APDs. Since the timing of $LaBr_3(Ce)$ is << 1ns, almost all of the timing resolution is contributed by the APD sensors and the electronics. The setup used for the timing is as shown in the Figure 8. Using this circuit, TAC spectra for a coincidence between the two APD+$LaBr_3(Ce)$ were obtained. The timing resolution for the APD was found to be about 1.6 ns (see Fig 9). We also realized the need to study timing spectra using a SiPM as these could be potentially useful device in the PET systems where energy resolution is not of very prime importance. For the SiPM, a TAC was generated using SiPM+$LaBr_3(Ce)$ in coincidence with a BaF_3+Photomultiplier. A timing resolution of 2.2 ns was obtained (see Fig 10) for this.

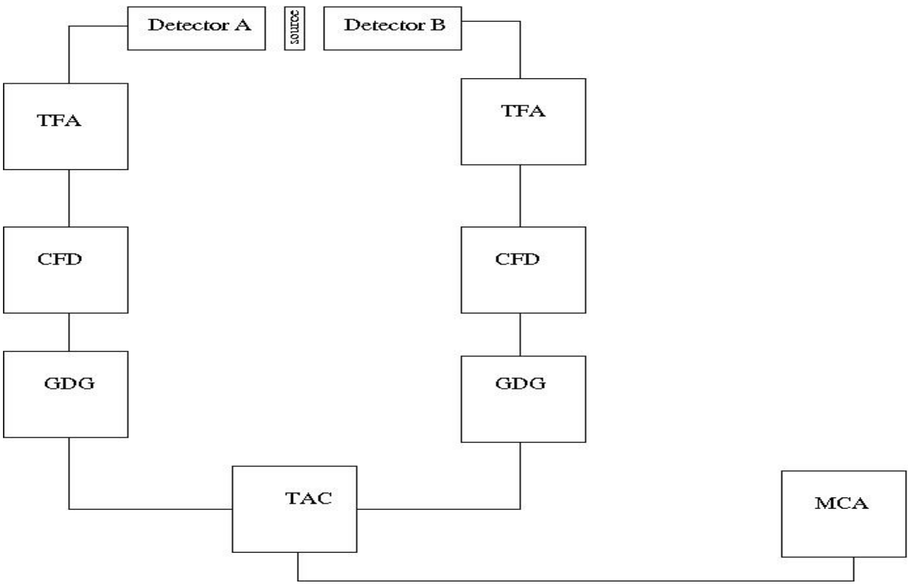

Fig 8: A general schematic representation of the set-up used for timing studies. The source used was 22Na generating two gamma rays of 511 keV emitted near back-to-back.

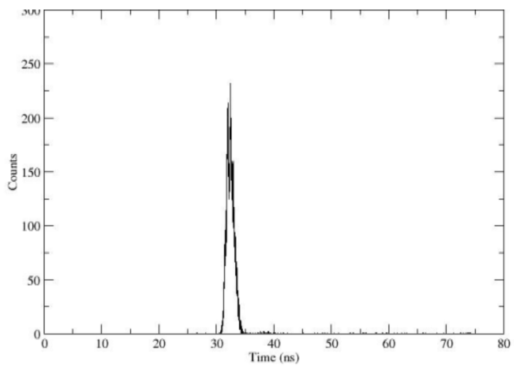

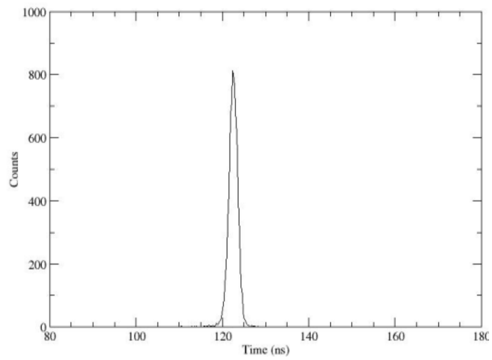

Fig 9: (left) TAC spectrum from coincidence between two Hamamatsu APDs (S8664). One of them was 5 x 5 mm while the other was 10 x 10 mm. A timing resolution of 1.6 ns was obtained. (right) TAC spectrum from coincidence between a SiPM + LaBr3, and BaF2 + photomultiplier. A timing resolution of 2.2 ns was obtained.

Investigation of SiPM at University of York: Over the last few years, the York group has been working intensively in the area of scintillator detectors for gamma-ray detection and novel photosensors such as SiPMs. Unusually, this interest strongly bridges the domains of nuclear physics and societal applications. Initially, funding as part of the GANAS consortium investigating scintillators and SiPMs for nuclear physics. The focus was on investigating the rapidly-evolving SiPM technology to establish its relevance to the task of collecting scintillation light from scintillation detectors both of standard technology – NaI(Tl) and CsI(Tl), and next-generation materials like $LaBr_3$(Ce). Following initial contacts with the Co. Durham-based detector company, Kromek PLC, the relevance of these developments to homeland security applications was identified. A short KTP was awarded by TSB (now Innovate UK) to develop a commercial product in a six-month time frame. This was successfully achieved and a product called SIGMA was launched by Kromek which comprised a hand-held gamma-ray spectrometer using a CsI(Tl) crystal coupled to an array of SiPMs. A variant of this device is now in a product called D3 which is a combined gamma ray and thermal neutron detection system. Kromek are presently delivering on an initial order of 1000 units of this system for the US government.

GEANT4 Simulations: The York group was successful in obtaining a mini-IPS award which aimed to upgrade and improve the performance of the SIGMA probe. This included full GEANT4 Monte Carlo simulations which not only explored radiation transport in the detector but also the full optical photon transport (see Fig. 10). The mini-IPS explored the segmentation of the scintillator crystal into sticks which better match the face area of the SiPMs. The individual detector channels need to be then combined.

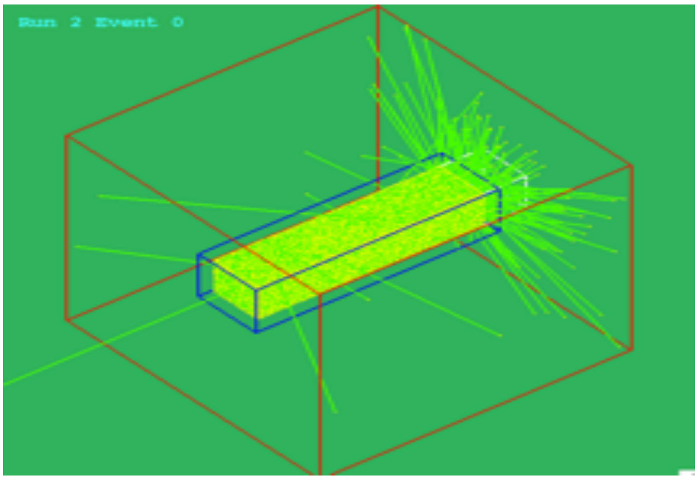

Fig. 10. Visualisation of transport of optical photons in a CsI(TI) crystal as part of mini-IPS project

The York group are also presently part of a consortium with Kromek and SensL (the SiPM manufacturer) who hold a grant from the US Defense Threat Reduction Agency (DTRA). This project has an ambitious goal for the target resolution of a future handheld spectrometer and can only be achieved with next-generation scintillator crystals such as $LaBr_3$(Ce), $CeBr_3$ or SrI_2. The coupling of SiPMs to these crystals has been explored and excellent results obtained, which are already highly competitive with that obtained using standard PMT technology. For example, Fig. 11 shows the quality of spectrum obtained for a 2" cubic LaBr3 crystal coupled to an 8 x 8 array of 6-mm SensL SiPMs; the energy resolution at 662-keV is 4.1 %.

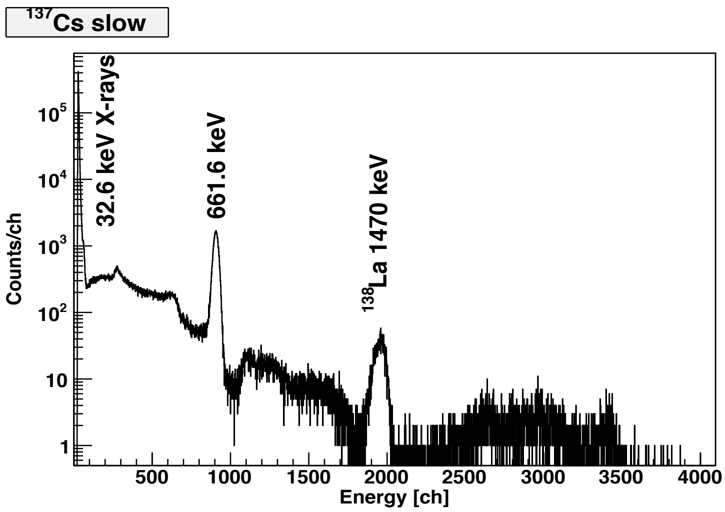

Fig. 11 Gamma-ray spectrum obtained with ^{137}Cs source for 2" cubic $LaBr_3$ crystal coupled to 8 x 8 array of 6-mm SiPMs

Most of the next generation materials are highly hygroscopic which means that they cannot be handled in ambient conditions. The award of £40k in funds from the Department of Physics at York has provided a low-humidity glove box system which can be used to safely handle these materials and bond them to SiPMs. The assemblies are then wrapped and canned in-house.

In the recent phase of the DTRA project, the glove box concept is taken to its logical conclusion, namely dispensing with the canning and coupling crystals and SiPMs in the glove box and carrying out all tests in a dark box within the glove box itself. This provides the ultimate flexibility in testing different configurations. Moreover, as SensL, the SiPM manufacturer are part of the DTRA project, it has been possible to ask them to develop their arrays to better match the demands of next-generation scintillators like $LaBr_3$. The first prototypes of the new arrays (J series) are becoming available at the time of writing. These have improved quantum efficiency for the wavelength range corresponding to the scintillators of interest as well as a much larger fill factor, using through silicon vias. It is expected that these new arrays will outperform PMT technology. An initial test suggests 3.3% energy resolution for a 1” $LaBr_3$(Ce) crystal coupled to SiPM array.

Investigation on the Energy Resolution of Scintillator Detectors using SiPMs at INFN Milano: Testing the SiPMs for High Energy Resolution Measurements

For the measurements two different kinds of SiPM were used in different combinations with $LaBr_3$(Ce) and CsI(Tl). Properties of the scintillation materials are shown in Table 3.

Table 3: *Properties of LaBr3(Ce) and CsI(Tl) scintillators in comparison*

Properties	$LaBr_3$(Ce)	CsI(Tl)
Density (g/cm^3)	5.08	4.51
Wavelenth of Max. Emission (nm)	380	540
Decay Time (μs)	0.016	0.68 (64 %), 3.34 (36 %)
Light Yield (ph/keV)	63	65

The first investigated SiPM consisted of an array of 4×4 elements, ArraySL-4. The Array has been connected to a 16-channel preamplifier board Array4-EVB-PreAmp. This preamplifier board was connected to an evaluation board Array4-EVB PixOut [8]. The second SiPM array that was used is the SensL B-series type single sensor. The tests are carried out with one, two and three sensors individually, and later on, to understand the response of a single SiPM, measurements were repeated for comparison with a standard Photo-multiplier Tube (PMT).

In the first stage, the SiPM ArraySL-4 was tested coupled to the CsI(Tl) crystal. The most suitable shaping time for the amplifier has been determined by testing different values with a ^{22}Na source. The best energy resolution of 7.08(1) % at 1.27 MeV has been obtained with 1 μs shaping. The corresponding spectrum of ^{22}Na and ^{137}Cs sources are shown in Fig. 12. The energy resolution at 0.662 MeV with the ^{137}Cs source was measured as 10.19(1)%.

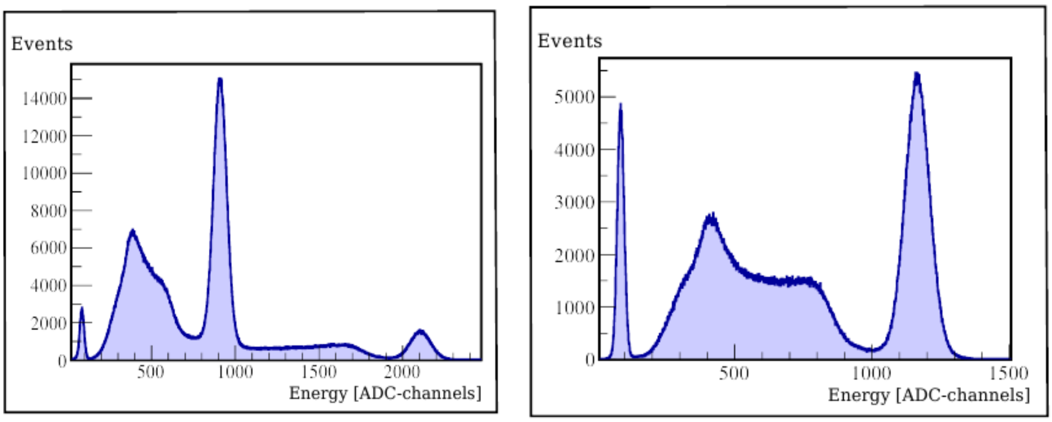

Fig. 12: *^{22}Na and ^{137}Cs energy spectrum with CsI(Tl) coupled to the SiPM.*

The ArraySL-4 showed a good response in these tests, similar to what one expects from PMTs and thus has the potential to be used as a light readout in gamma spectroscopy measurements. But further investigations were needed to determine the performance with high-resolution $LaBr_3$(Ce) scintillators and to study the pixel response since the aim is achieving the best resolution possible. Since the photon detection efficiency of ArraySL-4 SiPMs doesn't match well with the emission wavelength of $LaBr_3$(Ce), we changed the SiPM and used the B-series photo sensors to carry out the next tests. With a small 1 cm^3 crystal we obtained a comparatively good energy resolution and stable response in long measurements as well. Some modification of the preamplifier may be needed to fit it better to the required gamma-ray energy range.

The second part of the test was carried out by using a $LaBr_3$(Ce) crystal with a diameter of 3.7 cm and 3.7 cm length. As it was mentioned before B-series single SiPM sensors were used. They had a size of 6×6 mm^2 and 32% photon detection efficiency for the wavelength of the light emitted from our crystal. For comparison a regular PMT was used with almost 20% photon detection efficiency and 3.5 cm diameter.

The optimal voltage was tested for SiPM between 25V and 30V in 0.5 steps. As can be seen in Table 4, the best energy resolution was obtained at 28V. Therefore, this bias voltage was chosen for the tests carried out.

Since the area covered by one SiPM was very small compared to the surface area of the crystal, the energy resolution is rather modest (see Fig. 13). Therefore in the next step we measured the change of the energy resolution depending on the number of SiPMs coupled to the crystal (Table 5).

Table 4: *Characteristics of the large $LaBr_3(Ce)$ crystal with SiPM read-out.*

Voltage	Resolution @ 511 keV	Resolution @ 1274 keV	Peak Pos. (511 keV)	Peak Pos (1274 keV)	Counts in Peak BG substracted 511 / 1274
27	20 %	8,.4 %	114	280	6506 / 951
27.5	18.7 %	7.5 %	153	376	5278 / 767
28	17.6 %	7.05 %	196	485	4292 / 556
28.5	17.8 %	7.1 %	243	503	3523 / 442
29	18 %	7.2 %	282	690	2749 / 372
29.5	18,2 %	7.3 %	305	745	2443 / 331
30	18,5 %	7.55 %	350	855	2241 / 190

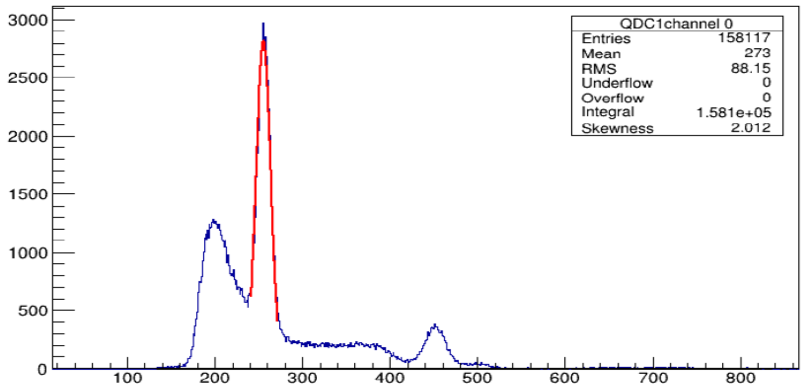

Fig. 13: *Energy spectrum of ^{22}Na in the case of only one SiPM coupled to the $LaBr_3(Ce)$ crystal*

Table 5: *Comparison of the response with varying number of SiPMs.*

Number of SiPM coupled	Resolution @ 511 keV	Resolution @ 1274 keV	Peak Pos. (511 keV)	Peak Pos (1274 keV)	Counts in Peak BG substracted 511 / 1274
1 (middle)	21.2 %	8.4 %	112	272	8588 / 1215
2	18.6 %	7.6 %	197	478	6590 / 825
3	14.2 %	5.7 %	294	715	2996 / 400

Indeed, as shown in Table 5 the peak positions, and thus the collected light scale roughly with the number of SiPMs, i.e. the covered surface area. Consequently, the resolution improves with the square-root of the area. It is interesting to note that the ratio of resolutions at 511 keV and 1274 keV indicates that this square-root dependence dominates the resolution, while the intrinsic noise of the system seems to be practicably negligible. On the other hand, calculating the photon statistics then points to an deficiency of about one order of magnitude in either the quantum efficiency of the SiPMs or the photon emission of the scintillator.

To find out which explanation is correct, the crystal was coupled to the regular PMT. To study the effect of the geometry, the whole surface of the PMT was covered by an aluminum 100% reflector tape with one, two and three windows in the exact size of the SiPMs opened respectively. At the end the full PMT window was opened.

Table 6 demonstrate a similar behaviour of the system as before with the SiPMs. The resolution strongly depends on the available surface area, and the resolution quoted by the crystal manufacturer can only be obtained with fully open coupling surface. Therefore it is concluded that indeed the number of photons obtainable for detection is about an order of magnitude smaller than expected for $LaBr_3$. Therefore, the investigations need to be continued with another crystal and/or with a SiPM array covering a larger part of the crystal.

Table 6: *Comparison of the response of a PMT with varying number of opening windows.*

Number of SiPM coupled	Resolution @ 511 keV	Resolution @ 1274 keV	Peak Pos. (511 keV)	Peak Pos (1274 keV)	Counts in Peak BG substracted 511 / 1274
1 (middle)	20.3 %	8.15 %	80	198	33223 / 3560
2	14 %	5.6 %	205	510	20131 / 2190
3	11.3 %	4.4 %	297	738	15166 / 798
Full opened	4.5%	1.88%	-	-	- / -

WP3 Pulse Analysis:

The work package WP3, as one of the central elements of GANAS, is concerned with the development of new methods for the digital pulse shape analysis for scintillation detectors. Special focus was the analysis of signals from multilayer phoswich detectors and background discrimination in large volume detector arrays. Within the project large sets of experimental data were generated at different sites. New algorithms have been tested already online and optimized for selectivity and efficiency. The analysis of those data sets allowed for the development of new powerful and fast algorithms that could be implemented already in FPGA based hardware typically used in modern experiments.

Phoswich detector with various combinations of material have been tested with gamma rays and charged particles. Advanced combinations of $LaBr_3$(Ce) and $LaCl_3$(Ce) performed extremely well while other combinations like LYSO/CsI(Tl) und CsI(Tl)/BC408 provide interesting properties for certain applications. Further, a new analysis method for the complex signals from CsI(Tl) was developed. This method called ***intrinsic Phoswich*** (iPhos) allows for a wide use for particle identification, to discriminate transmitted charged particles from those stopped in the detector material and for a very powerful background suppression.

The results have been discussed intensively in numerous meetings of the collaboration and most of them have been published in various articles and thesis. The technical developments of GANAS have become substantial part of the technical design reports for the CALIFA Endcap; approved by the FAIR management 25/08/2015.

The combination of a high resolution measurement of low-energy gamma rays and high-energy charged particles provides an extra challenge as the former would prefer the best and most expensive material in small pieces close to the sensor while the latter needs a very large absorption length. The phoswich concept allows for a full energy measurement for particles at higher energies but also the signal to background ratio is improved for gamma rays as the first absorber could be rather small. If the amount of light emitted from the different layers of scintillating material is detected by only a single photon sensor, the sum signal has to be has to be separated according to the different decay time constants of the different scintillators. Here pulse-shape analysis should provide a much cleaner separation than simple analogue filters.

New Algorithms for Phoswich Detectors

In case of the in-flight spectrometers discussed in this project, the combination of a high resolution measurement of low-energy gamma rays and high-energy charged particles provides an extra challenge as the first one would prefer the best and most expensive material in small pieces close to the sensor while the latter need a very large absorption length. The phoswich concept allows for a full energy measurement for particles at higher energies but also the signal to background ratio is improved for gamma rays as the first absorber could be rather small. If the amount of light emitted from the different layers of scintillating material is detected by only a single photon sensor, the sum signal has to be separated according to the different decay time constants of the different scintillators. Here pulse-shape analysis provides a much cleaner separation than simple analogue filters. For the detection of high energy gamma rays the additional layer can work either as an Anti-Compton shield or the information on the absorption depth could be used to validate certain reaction pattern. Detecting particles the multiple energy loss measurement is a very sensitive measure for the A/Z ratio of the ions and may be used for particle identification but also to distinguish stopped particles from those punching through.

To study the properties of different detector systems for protons at intermediate energies, an experiment was performed at the Centrum Cyklotronowe Bronowice (CCB - IFJ PAN) in March 2013. A proton beam of variable energy up to E = 230 MeV was scattered from a thin titanium target to be used in parallel for several different prototype detector operated by the collaboration.

Here a new developed phoswich detector made from 4 cm long $LaBr_3$(Ce) and 6 cm long $LaCl_3$(Ce) crystals was tested successfully. This detector with excellent properties [9] was developed from the collaboration partner IEM in Madrid together with the company St. Gobain. It was demonstrated that this combination conserves the excellent properties of both precious materials in the combination and signal amplitudes could be nicely separated [9]. Only the price of the special material and its hygroscopic property lead to limitations in certain applications. Also combinations of less fragile materials were tested for comparison. A phoswich made from a first layer of 1 cm CsI(Tl) and a second one of LYSO connected to a Hamamatsu S8664-1010 APD sensor was tested within the frame of a thesis [10]. As the light curves of both materials differ by more than an order of magnitude the two emissions could be easily separated. Protons of E = 95 MeV stopped in the active volume allow for an energy resolution of $\Delta E/E \leq 1\%$ (FWHM) while for transmitted protons a resolution of $\Delta E/E \geq 3.2\%$ (FWHM) was achieved which is limited by the multiple scattering. Important limitations for such concepts originate from the intrinsic activity and resolution of the LYSO.

Another mechanically very appealing approach would be the combination of high density materials like CsI(Tl) with organic scintillators like BC408. Also here the very different light emission constants look very promising but due to the very asymmetric efficiencies of those materials it turned out that this combination may be applicable to very specific applications only.

In all cases a new algorithm developed in the working group allowed for a very efficient, fast and hardware compatible separation of the interactions in the two different layers. This algorithm is based on the inversion of the amplitude matrices in separated time windows and could be derived analytically from the integrated light curves directly measured. For an optimized parameter setting the correlation elements were minimized and the diagonal elements maximized with respect to the signal to noise ratio. This major part of the computing could be performed for a calibration run offline. The algorithm itself was implemented for 16 channel in a single FPGA of the EPC3 family from Lattice together with the moving window deconvolution for the energy determination, different trigger methods and the full data handling part [MW16].

Signal shape based PID

Less expensive materials like CsI(Tl) or Na(Tl) have quite a good light output, but their spectroscopic resolution is typically limited by the intrinsic non-linearity. This is due to the fact that the light generation process depends on the ionization density the interaction generates in the cascade until it is absorbed. This property not only influences the total amount of light generated but also the population of states generating the light. Velocity and charge dependence of the electronic energy loss was already used in some experiments like the INDRA detector to separate particles and gammas. But especially at low energies the analogue methods had a quite limited resolving power.

The data set from the experiment mentioned above was very important to further investigate this properties in CsI(Tl) and showed that the proton gamma separation could be strongly improved by using numerical signal de-convolution. Additional data from an experiment at the LNS in Catania in 2012 were used to improve this separation down to energies below 1 MeV now. Here an E = 80 AMeV carbon beam produced a wide cocktail of light isotopes which could be stopped in 10 cm long CsI(Tl) detectors. Using a full Geant4 simulation and different models for the light production the contributions from delta electrons could be separated and a generalized model only depending on velocity and specific energy loss was derived [11].

In addition a new algorithm called the ***iPhos*** method [MB15] could be developed in the frame of a PhD thesis. The PID algorithm discussed before has shown that the absolute light emission together with the ratio of the fast and slow component of the light curve gives a clear fingerprint of the particle type and its average velocity in the material. Taking this into account the iPhos method provides a kind of $\Delta E/E$ measurement like a phoswich already in a single layer of material. Therefore, it got its name. It allows for particle identification, and the separation of stopped particles and particles not fully absorbed in the active medium. Using the difference in the correlation of fast and slow component of the scintillation, also a neutron - gamma separation is done. In addition, the consistency of fast and slow components also provides a strong handle for background reduction from reactions of particles in the detector material based on the same effect.
This finding became a fundamental part of the technical design report for the CALIFA Endcap [TDR-E] already approved by the FAIR management in 2015. Details of the method and the implementation in hardware are described in [12].

Investigation of ***the iPhos Method*** *with High Energy Protons (E ≤ 480 MeV):* Caused by the strongly reduced duty cycle of the accelerator facility at GSI another experiment using higher energy protons was performed at the Cyclotron of TRIUMF in Canada to test the stability of the iPhos method also at energies expected for the R3B experiment. We could show an excellent energy resolution of $\Delta E/E < 1\%$ even for large volume detectors made of CsI(Tl). Also precision data for the iPhos method were taken which allowed us to test a generalized model for the light production mentioned above and verify its dependency on particle velocity and type for this material also at large energies. This model was parameterized and included [13] to the simulation framework R3Broot which meanwhile is heavily used by the different groups. Using a segmented block of 3 x 3 x 2 detectors we were able to compare the pattern of nuclear reactions of the protons with the detector material with the R3Broot simulations to verify the efficiency and purity of the data sample after the iPhos separation. Based on this we calculated that the new method is able to suppress more than 95% of the background events in 220 mm long crystals without significantly changing the detection efficiency.

Dynamic Range: In many of the experiments planned, the in-flight spectrometers have to cover a very wide range of energies ranging from below hundred keV to several hundred MeV in the same measurement. While any dual range solution doubles the costs for electronics, the digital signal processing provides a good solution. Standard energy filters are quite well understood and their performance already gains 2-4 bits by the oversampling of the measured values at reasonable integration times. Due to the exponential decay of the signals from the preamplifier which are directly sampled, the higher amplitudes might be covered by the so-called Time over Threshold method (ToT).

This already well proven method was also tested in the experiments discussed above for the special preamplifiers (MPRB16 from Mesytec) optimized for the large capacities of the Avalanche Photo Diodes (APDs). With small changes in the filtering of the signals in this modules we were able to cancel all higher order terms in the signal decay. Already at an energy deposition above 10MeV the resolution of the TOT method reaches the one of the MWD. So it is possible to cover a range of more than 5 orders of magnitude using a single signal chain and a single digital data acquisition system.

System Development: One important fact in digital DAQ is that the amount of data has to be reduced as close as possible to the frontend electronics to limit the data sizes and computing power needed for the final analysis. So all the algorithms described have to be reduced and simplified to run on a compact and low power FPGA or DSP based hardware close to the detector. This needs an optimized hardware electronics design for this application but also special skills in hardware programming both available in the teams in this project. Parallel to the basic investigations on the algorithms described above, the electronics development and the prototype testing were performed in an ongoing process as the PSA has to be adapted step-by-step to the individual detector and hardware features.

For this development we had been using the FEBEX platform developed in the electronics division of the GSI in Darmstadt. This is a modular system with individual cards hosted in a 3U crate with a common interface to the Trigger and data acquisition computer. Each of up to 20 FEBEX3 cards in a crate hosts 16 channels of a 14 bit ADC at a maximum sampling rate of 50 MHz. A data stream of 11 Gb/s is processed in a single FPGA of the ECP3 family (Lattice) and such reduced to about 1 Mb/s on average. Within the project we managed to develop the full implementation of the pulse shape analysis features described before for all 16 channels in a parallel and dead time free way for each card. Including the full iPhos analysis, the energy reconstruction and a set of trigger and data handling features this provides a very cost effective, flexible and scalable solution for large scale experiments with a significant amount of detector channels but also for small scale applications in the lab. As described before this implementation was successfully tested in a number of experiments within the GANAS collaboration. Hardware programming is done in VHDL, a widely used language which allows for an easy porting of the functionality to most other hardware platforms.

WP4: Position Sensitivity in Large Crystals & Applications

WP4 addresses the development of technology needed to localize the interaction points of gamma-rays inside a large volume scintillator crystal and to set the basis for the construction of a position sensitive large volume scintillator detector for γ–rays of medium-high energy. The project requires the simulation, production and test of Position Sensitive prototypes which are capable to provide, on an event by event basis, the image produced by the scintillation light on the photocathode. Possible scintillators which can be used in the project are NaI, LYSO and LaBr3(Ce) [14-15].

Position sensitive gamma detectors are employed for a wide range of applications from physics research, bio-medicine to applications in the civil sector like oil investigations [16-17]. Determining the first interaction position of a gamma ray in a detector is important for high-resolution in-beam nuclear spectroscopy experiments to be able to correct the Doppler Broadening of the gamma lines [18-19]. This broadening occurs when the gamma ray source moves with high velocity and is caused by the angle dependent Doppler shift over the opening angle of the detector. The localization of the interaction point of the gamma ray inside the crystal and the tracking of the gamma ray while it is undergoing multiple scattering allows the correction for this effect.

With conventional thin (< 1 cm) scintillation detectors, the depth dependent response of the scintillation light arriving at the light read-out and the spatial distribution of the light along the crystal can be determined up to a resolution of a few mm. However, for gamma rays with high energies, the small thickness of the crystal reduces the detector efficiency significantly. Increasing the thickness of the crystal results in decreasing position resolution. Secondly, the crystals used in imaging applications like for example SPET have dark fully absorbing surfaces while gamma spectroscopy detectors must have reflective/diffusive surfaces. In fact, energy resolution is extremely important and all the scintillation light must be collected by the photo-sensors. These two aspects make the problem of the localization of the γ-ray interaction point inside the crystal much more difficult as position resolution is degraded by the thickness of the detector (Scrimger and Backer [20]) and the reflected scintillation light induces an extremely high 'background' which could cancel any position information [21-22]. It was already shown in Figure 1 of the first GANAS WP4 report that the percentage of photons which arrives on the photocathode (in the case of incident 662 keV γ–rays which have deposited all the energy in a 3"x3" LaBr3:Ce detector [21,23]) is approximately 10% in case of dark surfaces and 97% in case of diffusive surfaces. Namely, in spectroscopic crystals the surface-diffused photons constitute approximately 90% of the measured signal.

At the beginning of the GANAS project almost nothing was known on the imaging properties of position sensitive detectors that use several centimetres thick scintillator crystals and measure medium-high energy γ-rays. The GANAS project has stimulated a coordinated effort to start the R&D activity necessary to successfully tackle this topic. The project has, in addition, produced several published works and conference communications which would not have been possible without the GANAS project. It is also important to stress the synergy and the collaboration works between the different component of the GANAS collaboration. For example, two PSPMTs out of the four used in the tests done in Milano were lent by the Spanish group involved in other work packages.

Measurements of the 'integral' position sensitivity in a 3"x3" $LaBr_3$:Ce with a shielded spectroscopic PMT

This activity was focused on the study of the position sensitivity in a thick, cylindrical and continuous 3” x 3” (7.62 cm x 7.62 cm) $LaBr_3$:Ce crystal.

As a first step, a series of simulations were performed to check i) if the energy deposition of the incident gamma ray maintains the information on its original direction (the multiple hits inside the crystal and the consequent multiple light sources spots might degrade/cancel the positional information) and ii) if the scintillator light transport from the multiple light sources spots up to the photocathode still maintains the information on the original direction of the incident gamma ray. In fact, the diffusion on the surfaces of ≈ 85% of the collected scintillation photons might degrade/cancel the positional information.

Several gamma rays energies were simulated, i.e. 121 and 344 keV, corresponding to transitions of the ^{152}Eu source, 662 keV, corresponding to the ^{137}Cs transition, 1332 keV, corresponding to a ^{60}Co transition, 2.5 ,5 and 20 MeV. The left panel of Fig. 14 shows the distribution of energy deposited in the crystal projected on the x-axis of the photocathode when the gamma beam enters perpendicularly at the centre of the $LaBr_3$:Ce crystal surface (for symmetry reasons the projection on the y-axis is similar). It turns out that the distributions have a Gaussian-like shape centred around the source position. Similar results were obtained when the γ-ray beam was located at 1, 2 or 3 cm from the center (not shown), where the Gaussian was found to be cantered around 1, 2 or 3 cm from the centre, respectively. It is interesting to observe that most of the energy released is concentrated within one centimetre independently on the type of gamma interaction mechanism involved the various energies (photoelectric, Compton or Pair production). The right panel of Fig. 14 shows the percentage of energy released in the x range (-0.5 cm, 0.5cm) (open squares) or (-1 cm, 1cm) (full circles) as a function of incident γ-ray energy. The two plots clearly show that the γ-ray energy-deposition maintains the information on the incident γ-rays original direction.

In order to have an indication on how the diffusive surfaces affect the scintillation light distribution on the detection plane, we performed simple simulations using the code SCIDRA [24], in which the scintillation photons produced in the interaction process are transported to the photocathode. In the simulation, surfaces were assumed diffusive and the reflecting indexes of the crystal, the sealing glass, the optical grease and the phototube glass were taken into account. The resulting scintillation light distributions on the detection plane are shown in Fig. 14 for the gamma source positioned in the centre (x,y)=(0 cm, 0 cm)or in (x,y)=(2 cm, 0 cm), respectively. The spectra of Fig. 15 were normalized at x=-40 mm in order to emphasize the correlation between the gamma rays interaction position and the scintillation light distribution at the cathode. It turns out that in both cases there is no position sensitivity for gamma energies below 400 keV, due to the distance of the scintillation point from the detection surface. For larger energies the position sensitivity is clearly observed. This results indicate that gamma rays energy deposition does not cancel position sensitivity in a 3” x 3” $LaBr_3$:Ce crystal with diffusive surfaces.

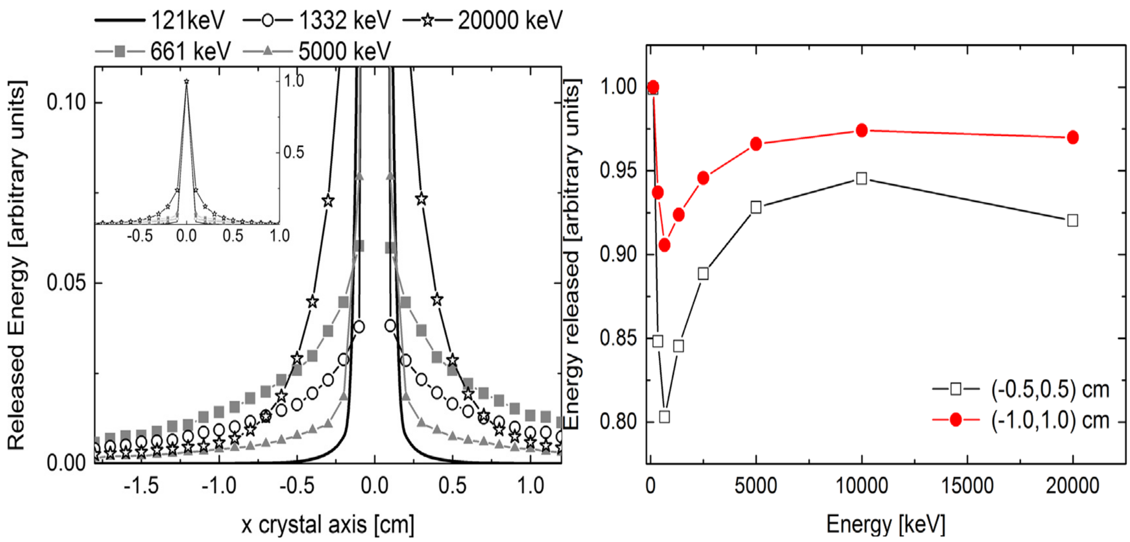

Fig. 14: Left Panel: The simulated released energy distribution projected on the x-axis is shown for several γ-ray energies. For all energies the maximum is set to one. The γ-ray beam is positioned in the origin. The scale of the y-axis is cut to 12% in order to better distinguish the different curve behaviours. The inset shows the full picture. The black line refers to 121 keV γ rays, the gray full squares to 662 keV, the open circles to 1332 keV, the gray triangles to 5 MeV and the open stars to 20MeV γ rays.
Right Panel: the percentage of energy released within the x range (-1 cm, 1cm) (full circles) or (-0.5 cm, 0.5 cm) (open squares) is shown as a function of incident γ energy. The γ ray beam is positioned in the centre of the front face [21].

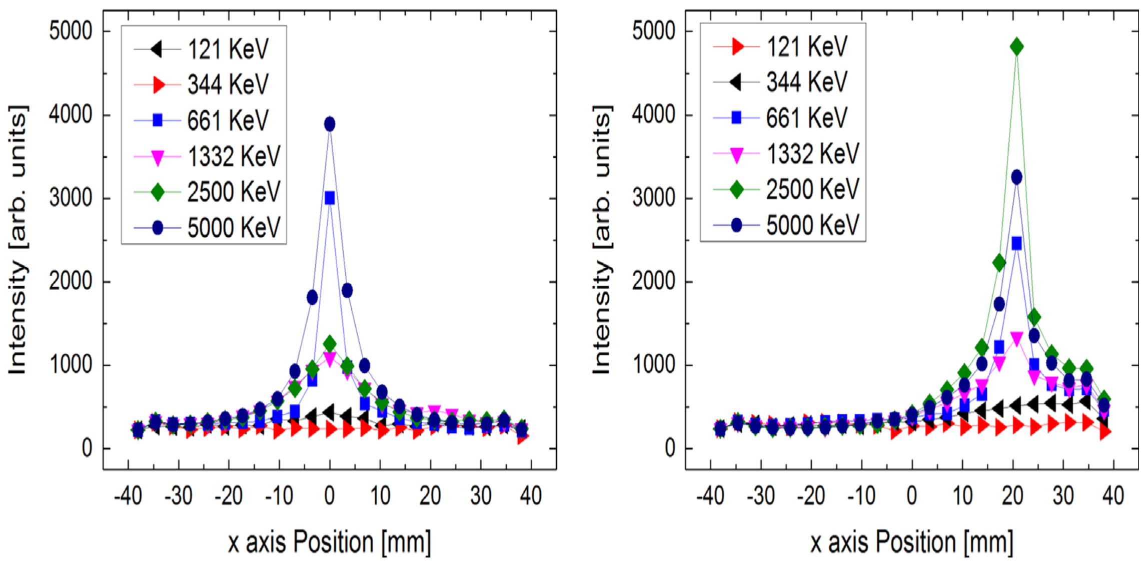

Fig. 15: Intensity distribution of the scintillation light as measured on the photocathode for gamma rays of energy from 121 keV up to 5MeV. In the left panel the source is in position (x,y)=(0 cm,0cm),in the right panel the source is in position (x,y)=(2 cm,0cm) and in both plots the curves have been normalized to have the same intensity at x=-40 mm [23].

The two plots of Figure 15 clearly shows that, for E > 400 keV, the transport of scintillation light to the PMT cathode slightly degrades but does not cancel the positional information.

The conclusion of this preliminary part of the work is that it is possible to achieve position sensitivity in a 3"x3" $LaBr_3$:Ce scintillator if PSPMT (or in future SiPM composite sensor) would be used. In fact, neither the γ-ray energy deposition nor the transport of the scintillation light destroy the information on the direction of the incident radiation. This is a key information which has provided the starting point for the following part of the project more dedicated to measurements.

At first, the position sensitivity was studied using a 1 mm collimated beam of 662 keV gamma rays from a 400 MBq intense ^{137}Cs source and a spectroscopic photomultiplier (HAMAMATSU R6233-100SEL). The PMT entrance window was covered by black absorber except for a small window 1 cm x 1 cm wide (see Figure 16).

Fig. 16: The photo shows the $LaBr_3$:Ce crystal and the shielded PMT. The window is at 1.5 cm from the center along the x-axis [21].

The PMT used has a cathode luminous sensitivity of 148 μA/lm and a cathode blue sensitivity index of 16.1. The PMT was coupled to an HAMAMATSU E1198-26 voltage divider(VD). The detector is commonly used in nuclear spectroscopic measurements, with a typical energy resolution of 20 keV (FWHM) at 662 keV, which corresponds to the value of 3% quoted in the Saint Gobain detector data sheet.

In this part of the work, the measurements that have been performed were not on an event by event basis but 'integral', namely for each position of the collimated source an energy spectra was acquired. A complete scan of the detector over a 0.5 cm step grid was performed for three positions of the 1 cm x 1 cm PMT shielded window. For each configuration the Full Energy Peak centroid, its FWHM, area and peak asymmetry of the 662 keV gamma transition were analysed.

We have found that the most effective full energy peak property to identify the position of the gamma ray interaction point turns out to be the peak centroid position. The peak asymmetry and the peak FWHM did not present a strong correlation with the position of the collimated γ-rays beam [21].

This work has shown that the full energy peak centroid is a position sensitive quantity. Look up tables associated to a window located in few different positions can be used to retrace the gamma-ray source position. In particular:

- The light collected in the centre of the crystal gives a radial information on the position of the γ source.
- The light collected at the edge of the crystal on the x or y directions gives a precise information on the x or y coordinate, respectively.
- By combining the information of only three windows positions one is able to estimate with good precision the position of the gamma source. The light collected at an intermediate radius from the crystal centre do not seem to bring relevant information. The reason of this has to be further investigated.

In the second stage of the work we used 4 Position Sensitive PMTs (PSPMT Hamamatsu H8500) coupled to the surface of one 3" x 3" $LaBr_3$:Ce. The crystal, the same used in the tests previously discussed, has diffusive surfaces and the 4 PSPMT were placed to fully cover one surface window. Each PMT has dimensions 2”x2” and consists of 64 segments.

The four available PMT’s were not all equal: two of them had 10 dynodes and a bialkali photocathode, while the other two had 8 dynodes and SBA photo-cathodes. The performances of the two types of PMT’s were different: the energy resolution of each single PMT coupled to the crystal was about ~ 5 % for the first type and about ~ 4% for the other. When used together, the energy resolution was ~ 4.5% at 662 keV. The complete coverage of the detector surface implies the use of approximately 120 segments. In order to have a simpler setup, we short circuited segments in groups of 16, so to end up with 12 macro active segments. Note that, since the single segments have in principle different light response, short circuiting a group of segments reduces the possibility of optimizing the performances of the PMT’s.

The data were taken using a ^{137}Cs source with 400 MBq intensity collimated in a 1 mm diameter beam spot. High voltage of -900V was applied to the PMT’s through a CAEN N1470 4 channel HV power supply. Data were taken using two 8 channels in house built units, and a KMAX based DAQ system. The source was placed in several positions and the measured coordinates of each event were obtained calculating the center of gravity of the light distribution [31]:

$$x_{pos} = \sum (x_i * Q_i) / \sum Q_i$$

where x_{pos} is the x-coordinate of the position, x_i are the x-coordinates of each segment and Q_i are the collected charges in each segment. A similar equation is used for the y-coordinate y_{pos} .

Gating on the 662 keV transition, in an event by event approach, the position profiles are Gaussian distributions with a FWHM of about 2.3 cm. In Figure 17 the profiles on the x and y axis (cathode plane) corresponding to two source positions 4 cm apart in the x direction are shown. If we plot the centroids of the distributions as a function of the source position, we see a deviation from linearity which can be however corrected with a 3rd degree polynomial.

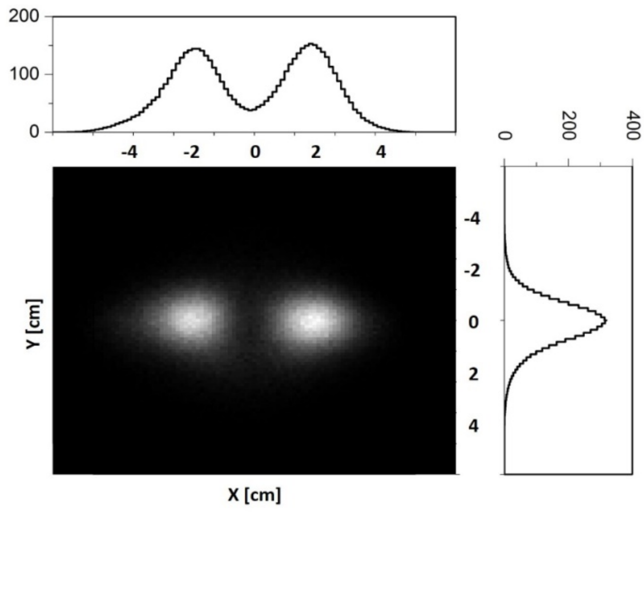

Figure 17. The central plot shows the two-dimensional image corresponding to two source positions 4 cm apart in the x direction. On the top and on the right, the profiles on the x and y axes are shown, respectively.

As the interest of this work lays in large crystals and in the possibility to detect high energy gamma rays we investigated the position sensitivity of the 3”x3” crystal for gamma rays of 1836 keV from a ^{88}Y source. Since the final goal is the possibility to correct for Doppler broadening in inverse reactions, we are only interested in the position identification in the x-direction. Therefore, we collimated the source with 20 cm lead, leaving a window 5 cm high and 1 cm wide, and performed two measurements with the source in the window centre at (x,y) = (-1.5 cm, 0 cm) and (1.5 cm, 0 cm), respectively, with respect of the crystal centre. The FWHM of the Gaussian was 2.2 cm, similar to the one measured for the 662 keV of ^{137}Cs (2.3 cm) shown in Figure 4. We have therefore verified that i) the used Pb collimation system built for the 1836 keV radiation (see Figure 6) effectively collimate the gamma-rays and that ii) position sensitivity is present at both 662 and 1836 keV.

In order to investigate whether this position resolution would be sufficient to correct for the Doppler broadening, we performed the following measurements: the ^{88}Y source was shielded by 20 cm Pb leaving a 1 cm wide opening, as shown in Figure 18, and a set of measurements were performed with the detector shifted in 1 cm steps along the x-direction. The detector surface was covered by 6 measurements. The live time was the same for all measurements. The total energy resolution for the 1836 keV transition was 50 keV.

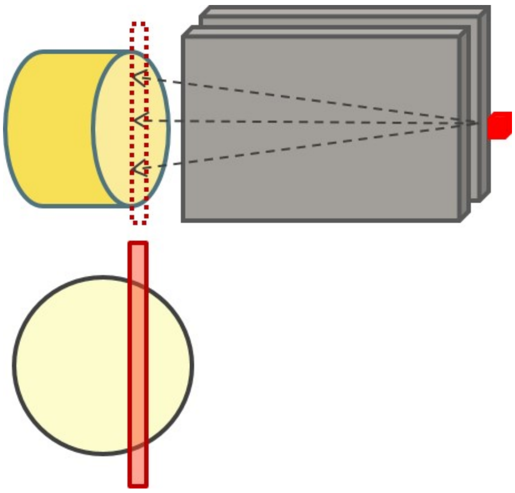

Figure 18. The figure shows the setup used for simulating a Doppler broadening effect: the 88Y source was shielded by 20 cm Pb, leaving a 1 cm wide opening, and the detector was moved in 1 cm steps along the x direction.

We then recalibrated each set of data assuming a moving source with v/c=0.5, with the detector placed at 20 cm distance and at 90° with respect to the source direction. The energy corresponding to the 1836 keV transition would range from ~1500 keV for forward angles to ~1700 keV for backward angles in the lab system. Recalibrating each set of data and summing up the data, a spectrum was obtained which simulates the effect of Doppler broadening in an inverse reaction experiments, the measured width of such a peak structure is ~ 250 keV. For each event the interaction position of the incident gamma rays was estimated and the gamma-ray energy corrected. The resulting 1836 keV peak, after the event by event Doppler Broadening correction, has a Gaussian-like line-shapeand a FWHM of 100 keV. It was therefore possible to reduce of a factor 2.5 the FWHM of the 1836 keV full energy peak.

Simulations of light propagation in scintillator detectors: The investigations of light response for gamma rays performed in Kraków in comprised simulations of light propagation in detectors of different sizes.
Using GEANT4 Monte Carlo software the propagation of light produced by gamma rays in scintillation detectors have been simulated for two detectors: cubic $LaBr_3$ crystal (2"x2"x2") and PARIS phoswich detector $LaBr_3$ (2"x2"x2") / NaI (2"x2"x6"). The light responses for the 1 MeV gamma rays emitted into the center of the crystal or into the left side position have been calculated for each detector.

The obtained light response of cubic $LaBr_3$ crystal (2"x2"x2") for 1 MeV gamma rays presented, in Fig. 19, shows the possibility of the interaction point discrimination by the light output. The differences visible on Figure 19 (left and right panel) indicate the possibility of obtaining precise gamma energy deposit information by usage of segmented photodetector.

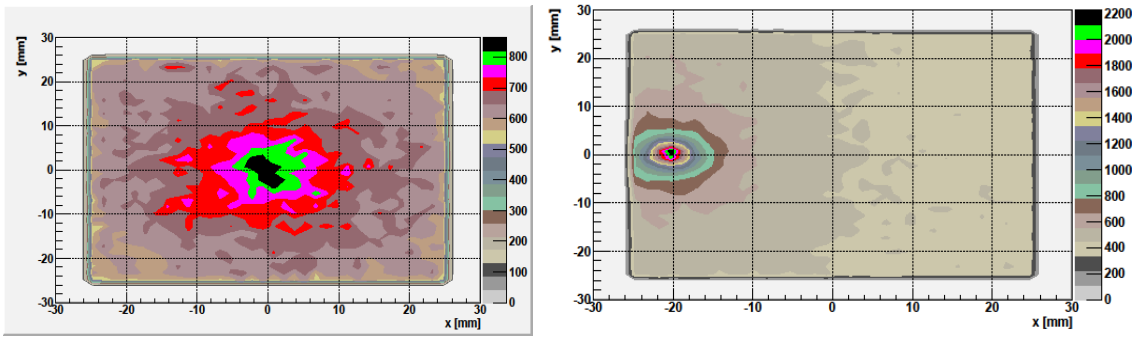

Fig.19 Distribution of scintillation light measured on back side of cubic 2"x2"x2" $LaBr_3$ crystal. The scintillation light was produced using 1 MeV gamma-rays collimated beam: left panel - the gamma beam was collimated in the center of the $LaBr_3$, right panel - the gamma beam was collimated at the left side of the crystal (point x,y = [-2 cm, 0]).

In the case of response for 1 MeV gamma rays of phoswich detector, composed of 2"x2"x2" $LaBr_3$ connected to 2"x2"x6" NaI, simulation results show no dependence on the interaction point. Obtained results presented in Fig.20 for this detector are very similar for different irradiation (into the center and to the side). They indicate that there is no possibility to get information of the energy deposit positions by measuring the scintillation light distribution.

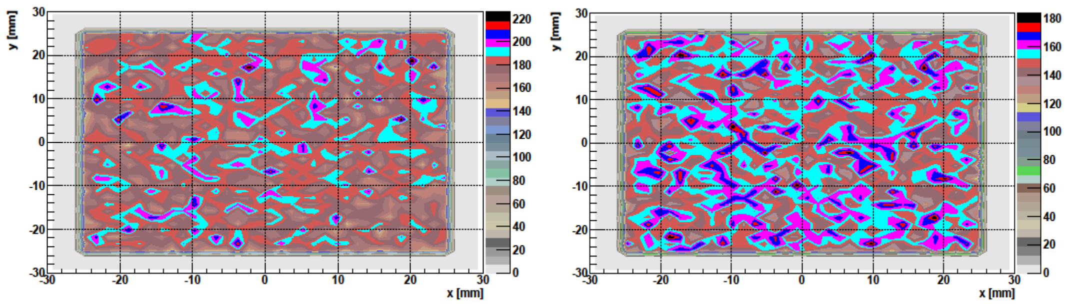

Figure 20. Distribution of scintillation light measured on back side of phoswich detector (2"x2"x2" $LaBr_3$ + 2"x2"x6" NaI). Scintillation light was produced by absorption of 1 MeV gamma ray, which was emitted: left panel - into the center of the $LaBr_3$, right panel - into left side (point x,y = [-2 cm, 0]).

The information on energy deposition position using the light measurement depends mainly on length of detector and is not possible for longer phoswich detector ($LaBr_3$+NaI). Due to longer path of light from the gamma interaction point to the photodetector information on interaction point is lost.

These measurements confirm that in general, for imaging application, the surface of the crystal should not be shorter than the length.

The 3D Position sensitivity in a cubic 1.5" x 1.5" LYSO crystal coupled to 6 PSPMT

Further, it was investigated the 3D position resolution of a thick scintillation crystal employing a novel approach different to that used in usual gamma cameras. In general a gamma camera consists of one or more flat crystal plates coupled to a single position-sensitive photomultiplier (PMT) or to an array of PMTs and one can investigate the interaction position in the material in 2D by analyzing the light distribution created. Depending on the depth of the interaction position the width of the light distribution will vary. Interactions closer to the PMT surface would have less spread light at the photo cathode than those interactions further away

In our approach, a single large volume cubic crystal is used and coupled to Position Sensitive Photomultiplier Tubes (PSPMT) on all the sides of the crystal. This solution, aimed to get the position information in 3D. We tested for large crystal volume the limits of such a 3D camera and the effect on the created light cloud that is optically transported to the photocathodes. It is verified that different interaction points have a different response in the detector signal.

Design of the Detector: The choice of detector material is of major importance. For spectroscopic purposes the energy resolution must be high and the efficiency large. Therefore $LaBr_3$ or $LaCl_3$ would be prime candidates. However, the high cost and handling problems due to hygroscopy prevented us using these materials. For the aim of our investigations a large light yield is already sufficient and LYSO was found to be suitable. We thus studied the response of a scintillation gamma camera using a cubic, polished surface and Cerium doped, inorganic Lutetium Yttrium Oxyorthosilicate (LYSO:Ce) continuous crystal with a size of 3.4 x 3.4 x 3.4 cm^3. The scintillation properties of the crystal are shown in Table 7. The only drawback is that Lutetium contains a radioactive isotope with an abundance of 2.5 %, which decays into excited states of Hf causing self-activity radiation.

Table 7: Optical properties of the LYSO:Ce crystal

Density (g/cm^3)	7.4
Index of Reflection	1.82
Decay Constant (ns)	44
Light Yield (ph/MeV)	32.000
Emission Wavelength (nm)	420
Energy Resolution (511 keV) (%)	25

In this work six PSPMT were used. All the faces of the cube were covered with a Hamamatsu H8500C model multichannel photomultiplier tube. The H8500C has square shape and an external size of 52x52x28 mm^3, a sensitive photocathode are of 49x49mm^2 The photocathode is bi-alkali and has a 12 stage metal channel dynode that is used as electron multiplier with a gain of about 10^6. A 64 channel multi-anode assembly is done with 8x8 matrix anode pixels.

The 64 channels of a PSPMT were not used individually, but four quadrants were defined by connecting together 16 channels each. An electronic circuit was built to obtain signal amplitudes proportional to x- and y-positions in the reference frame of each PSPMT by generating conventional difference over the anode sum signals. In this way the number of the signals to elaborate was reduced and the read-out was simplified.

Since the dimension of the crystal is smaller than the PSPMT window, for the coupling of the crystal to the PSPMT a plastic bridge is used. Six plastic light guides are coupled optically with the special glue that improves the light collection and minimizes the surface effects on each surface. The complete system then was covered with black tape and measurements were taken in a dark area to reduce the noise due to possible light leaks. The set-up is illustrated in Figure 21.

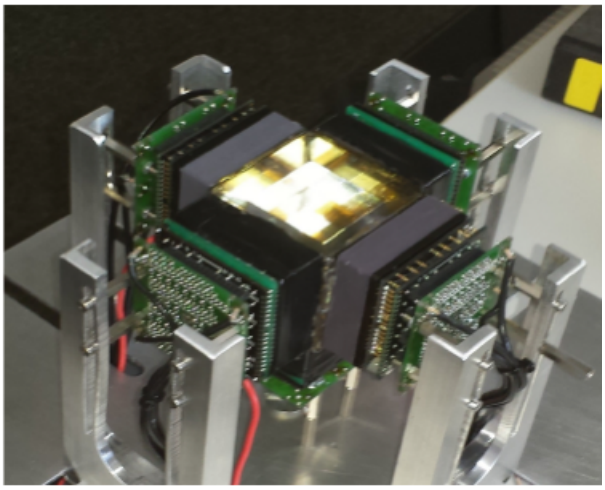

Fig. 21: Picture of the detector system with one surface open. The crystal itself can be seen in the middle covered with plastic windows coupled to PSPMTs. The open surface was covered later.

Since position determination is defined by individual quadrant read-out of the PSPMTs, equal gain on each channel is important in order to construct the path of light in the volume correctly. For the gain matching, each surface was illuminated homogeneously with gamma rays under the same conditions. To illuminate the full crystal surface, a non-collimated source at a suitable distance was used.

To discriminate unwanted self-activity events due to the intrinsic radioactivity of the LYSO crystal, an external reference detector was employed in the setup and a ^{22}Na source was to provide a coincidence in both detectors. As reference detector a cylindrical $LaBr_3:Ce$ crystal with 1.5 inch diameter coupled to a HAMAMATSU H2431-50 PMT was used. The source was placed in front of the gamma camera. The ^{22}Na source was chosen since it is a positron emitter that produces two 511 keV annihilation gamma-rays in opposite directions. One was detected in the LYSO crystal whereas the second one was detected in the reference detector generating a trigger condition for the data acquisition. This assures that all 24 channels (4 from each side of the cube) are then calibrated by 511 keV gamma rays without background from self-activity or environmental background radiation. Absorption and scattering of the gamma rays in the PSPMT and the associated signal read-out circuitry is negligible in first order.

After the gain calibration, the ^{22}Na source was collimated with a pyramidal 8 cm thick tungsten collimator, placed at the front face of the gamma camera window. The coordinate system is considered individually for each side of the cube. The center of each surface is taken as (0,0,0) in (x,y,z) formalism, directions are chosen as shown in Figure 22. We investigated how the amplitudes of the channels differ by moving the source across the x/y-plane in steps of 5 mm. Due to the symmetry of the scintillator cube and the light read-out set-up, scanning the detector from one side already reveals the full response in 4π.

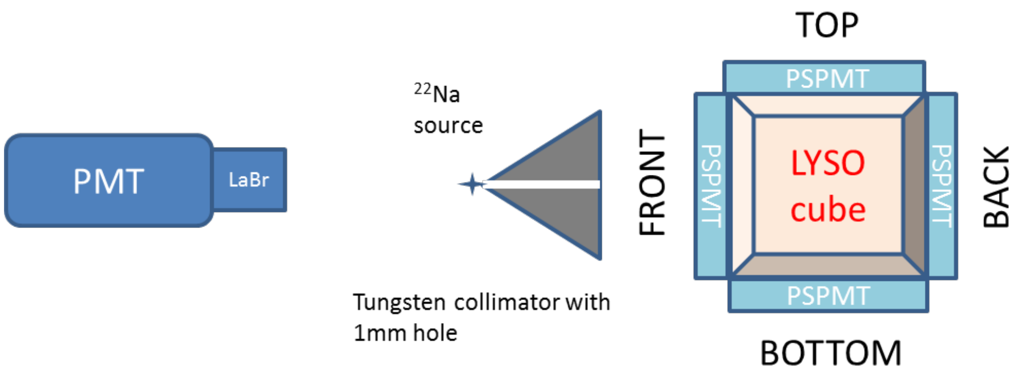

Figure 22: a) Schematic of the experimental setup (not scaled).

In this measurement the LYSO detector is biased around -800 V for each PSPMT by adjusting their gain with respect to the 511 keV gammas. For fully absorbed gamma rays anode signals have an amplitude of -80 mV and dynode signals (used for time reference) have an amplitude of 20 mV. The raw anode signals are amplified by two different 16 channel fast amplifier CAEN N979 NIM modules. After the amplification, fast signals are delayed by 500ns before they are fed into V792 QDC (Charge to Digital Converter) modules. The dynode output signals from the PSPMTs are sent to a timing filter amplifier and then to a leading edge discriminator from LeCroy, model 623B. All the channels are set to the same threshold value, the AND of the discriminator signals were fed into a coincidence module together with the logic signal of the reference detector. The QDC gate is created from the coincidence signal. Each signal from PSPMTs, 4 from each surface of the cube, are set in OR condition. With this trigger condition data is collected by using a Multi Branch System (MBS) data acquisition system of GSI, and offline analysis was performed via the GSI Object Oriented Online Offline system Go4 and the ROOT data analysis framework.

With a coincidence trigger condition, measurements were taken for 20 minutes acquisition time for each source position. This resulted in typically about 300 events per position. The different amplitudes of the QDC signals correspond to the different amount of measured light on the cube surface depending on the source location. An example for the raw data is shown in Figure 23 for the condition when the source is placed at the right-top corner (-15,+15). The four histograms of each line correspond to one surface, from top to bottom it is aligned as Front, Right, Back, Left, Bottom and Top surfaces of the cube.

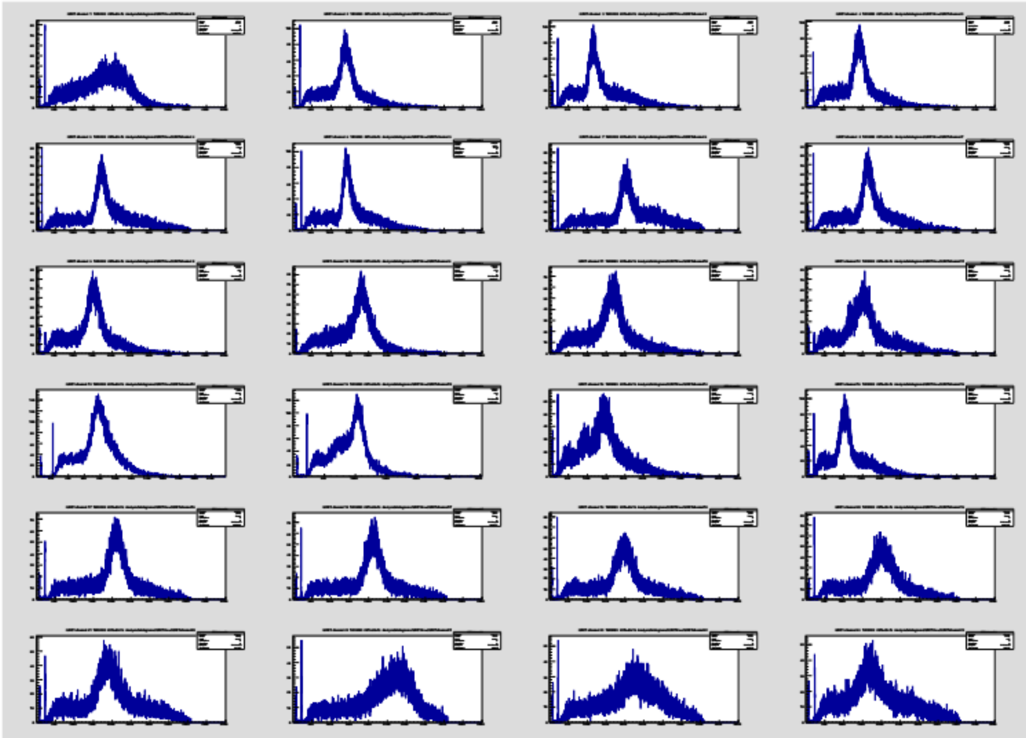

Figure 23: Signal distribution of each anode depending on the source position in front of the detector.

These amplitudes are then used to construct the interaction position. The resolution estimation is derived from Gaussian fits of the reconstructed profiles. How it is applied to get this construction will be explained later in this report in the interaction point determination part.

In the analysis an energy gate at around 511 keV was set in the reference detector spectrum and in the sum spectrum of the cube detector. The time resolution of the set up was determined separately for each PSPMT on six sides to 9 ns resolution and a time gate was applied to reduce random coincidences and background events. Applying all the demanded conditions, a substantial improvement is seen.

Interaction Point Determination: The algorithm that is used to determine the interaction position is based on a mathematical model considering the charge collection on anodes which was published by H.O. Anger and is still a basic principle of image reconstruction. The principle of the logic is illustrated in Figure 24. The Anger formula calculates the position of the event as a mean value of the measured charge distribution, which represents the light distribution in the imaging plane depending on the source position assuming a constant amplification of the photomultiplier tube.

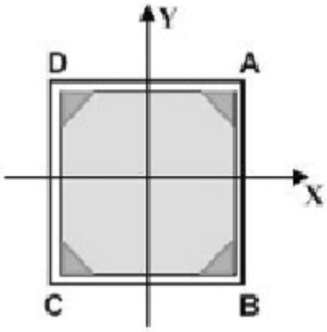

$$X = \frac{(A+B)-(C+D)}{A+B+C+D}$$
$$Y = \frac{(A+D)-(B+C)}{A+B+C+D}$$

Figure 24: Schematic surface of the PSPMT with quadrants labelled as A, B, C, and D. On the right, the standard algorithm is depicted.

We applied this formula by using the amplitudes we get from the quadrant contacts. The 2D (x/y) information was taken from the front and back surfaces while the left, right, bottom and top surfaces of the crystal were used to obtain the depth (z) information. Figure 25 shows as an example the depth distributions obtained for the scan positions (15,15) and (15,10). Due to the reduction of the remaining gamma intensity by absorption in the preceding layers of the crystal, the intensity drops for deeper layers, resulting in the observed asymmetric shape. The distribution is in first order independent of the scan position. However, we used the depth information from the side closest to the x/y scanning line for ultimate depth resolution. Selecting different depth regions by applying cuts on the depth distribution helped to improve the position resolution in x and y.

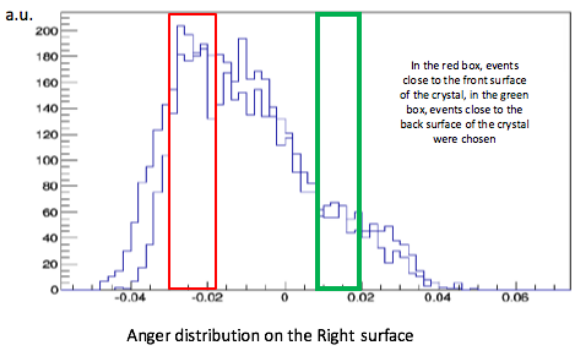

Figure 25: Projection of the depth distribution for two different positions of the source from the "right" surface of the crystal. Since the origin of the coordinate system lies in the center of each surface (0,0,0), negative values correspond to the side where the gamma ray enters the cube.

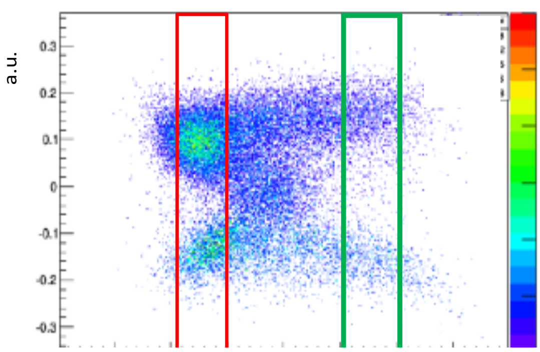

Figure 26: (x,y) correlation for two different positions of the source (15, 15, 0) and (15, -15, 0). Depth information is taken from the right surface of the crystal. The distribution shows the distribution of the 511 keV gamma-ray in the crystal. No depth cut was applied to show the full

The x- and y- position distribution of the collected light at different source positions are shown in figure 13 when the source is at (15, 15) and for the one below, the source was moved along the y axis and placed to (15, -15).

To get the optimal resolution from the front surface of the crystal, we take the projection of the correlation in Figure 25 onto the y-axis by applying gates on the side surfaces, depending on the interaction depth of the gammas resulting in the image shown in Figure 26. The position axis is given in “Anger” units. The position resolution in this example transformed into a length scale is ca. 7 mm FWHM.

As shown in Figures 27,28 the distribution of the light is rather symmetric in case of centrally detected gamma rays, while the distribution gets distorted in the case of a light cloud positioned near the edge of the crystal, this is interpreted as pin-cushion effect producing systematically shifts towards the centre of the image reducing the position resolution.

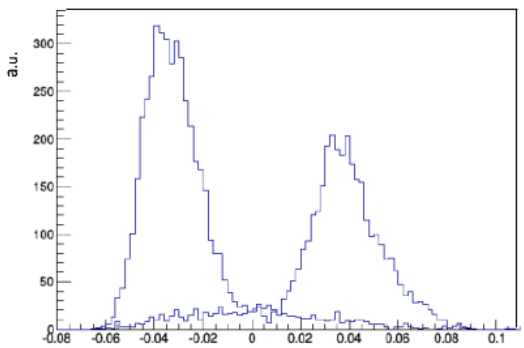

Figure 27: γ-distribution for two different positions of the source close to the front of the crystal.

Undesired effects on the edges because of a non-linear response were seen during the measurements. Even if the light reflections at the edges were perfectly uniform, the boundaries will widen the light distribution and shift the centroid of the light far from the real interaction position.

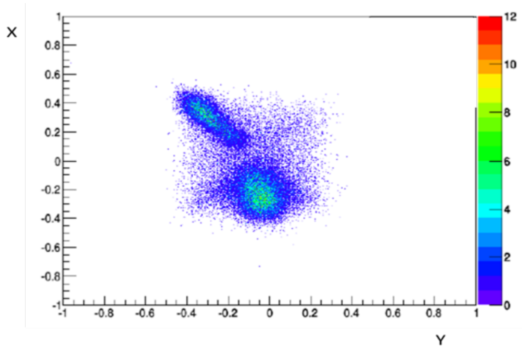

Figure 28: Positioning image from the front face of the detector. It is the comparison of two interaction points, on the corner edge of the crystal and close to the middle of the crystal. An edge effect on the measured light distribution is clearly seen.

Finally, to get the spatial resolution distribution across the crystal, measurements were taken by moving the source in 5 mm steps in x and y. X-Y distribution which represents the interaction points were observed at the back and front surfaces. For the 3D imaging, depth information was used by applying cuts along the z direction of the crystal as it is seen in Figure 29. Here, spatial resolution for two different cuts across the crystal for the front (red) and for back surfaces (green) of the cube were presented. As it is seen, the spatial resolution along the crystal is not homogeneous. The cut on this region was applied to all the surfaces carrying the z information. In Figure 29, the same procedure was applied by using the green cut seen in Figure 26, and the projection this time was taken from the back surface of the crystal. In both cases the resolution obtained for more central scan positions fluctuates around 0,3 cm while it increases towards the edges. This effect is more prominent for interactions in the back part of the crystal. It can be attributed to the pin cushion effects discussed above, but may also reflect pixel gain variations of the PSPMTs and inhomogeneous light absorption due to variations of the crystal surface qualities.

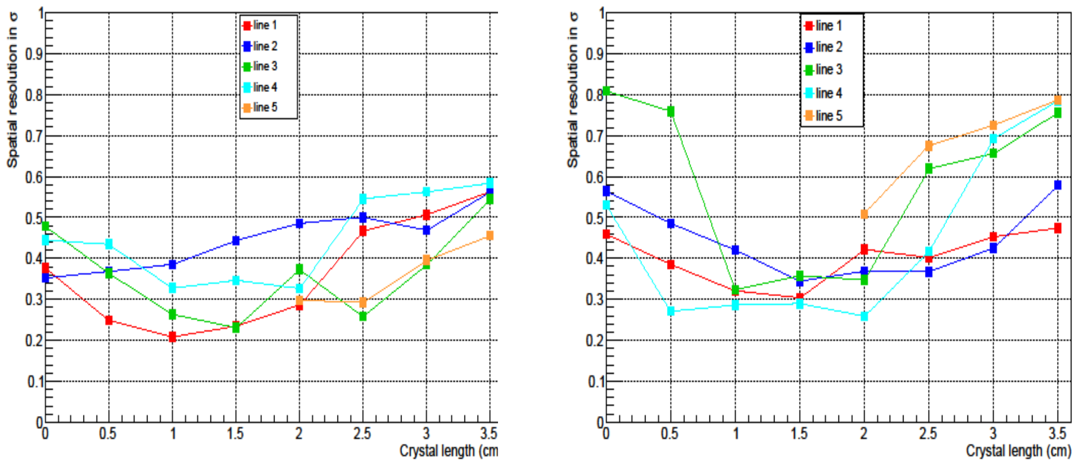

Fig. 29: Position resolution distribution across the front surface of the crystal

Conclusion drawn: The light distribution of a cubic LYSO scintillation crystal with 3.4 cm side length and the position sensitivity depending on the interaction position of gamma rays was studied. Employing the Anger formalism with corrections for the interaction depth an average resolution of 8 mm (FWHM) was obtained. The results demonstrate that the new approach indeed provides position information in 3D. The limitation in resolution comes mainly from pin-cushion effects. A way-out might be individual anode pixel gain calibrations and fitting of theoretical light distribution curves. Optimizing the surface treatment may also be important to improve the resolution further.

WP5 Segmented scintillator:

The experiments at the new radioactive ion facilities, FAIR and SPIRAL2, require innovative detectors systems, including very efficient gamma-ray arrays or calorimeters, which can be used for the simultaneous detection of high-energy photons with relatively good energy and timing resolution, multiplicity and an sufficient summing of the low-energy gamma transitions. In addition, the discrimination or measurement of energetic charged particles, is important. For experiments where the source of gamma rays is moving, as is the case for most of the planned experiments, a relatively good determination of the first interaction position in the scintillator is needed, in order to make the Doppler correction of the gamma-ray energies. One can achieve such a goal by using novel scintillating materials (see WP1) and by adopting gamma-ray tracking methods. All of this requires implementation of segmentation of the calorimeters both in the tangential (x,y) and radial (z) directions or other means to determine interaction positions in 3D. The objective of this Work Package was to investigate and develop prototypes of such segmented gamma detection arrays.

In the design of CALIFA's forward endcap an innovative solution using two scintillator crystals stacked together one after the other in a so called Phoswich configuration with only one common readout is being considered the so called CEPA (Califa Endcap Phoswich Array). Combining two materials one can distinguish at what depth the impact happens. The second layer is used to fully absorb the gamma energy or in the case of first hit in the second layer to veto that specific event. For protons, a two-layer configuration is also useful in order to determine the initial energy. Instead of using one very long crystal it is possible to determine the initial energy from the energy loss in two shorter crystals. In the choice of scintillator material one has to take into account that the crystals are optically compatible i.e the second layer crystal has to be transparent to the light emitted by the first layer. During 2012-14 a full characterization and evaluation of this Phoswich approach was performed.

The first prototype; 1” Al-cylinder with 3cm $LaBr_3$(Ce) stacked with 5 cm $LaCl_3$(Ce) crystals closed by a 4mm glass-window and coupled to a single Hamamatsu PM-tube was tested first at CMAM (Fig. 30) for high energy gamma rays, where a standard NIM electronic set-up was used and secondly with high energy protons at the Svedberg Laboratory in Uppsala Sweden.

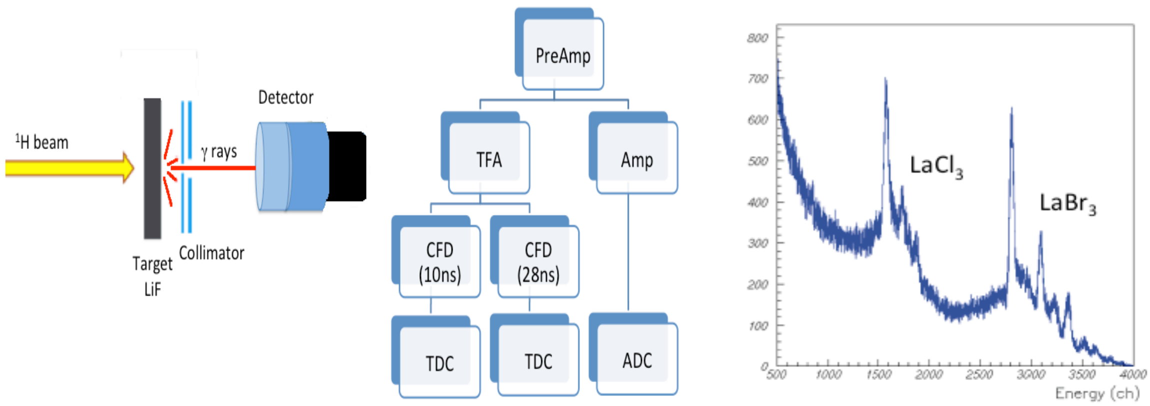

Fig. 30 The CMAM experiment p+^{19}F→gamma, electronic set up and resulting gamma spectrum. Due to differences in light yield the gamma stopped in the $LaBr_3$(Ce) show up at twice the channel number.

At Uppsala a low intensity proton beam at 180 MeV was provided by the Gustaf Werner Cyclotron and collimated to a few millimeters. An annular degrader of 25 mm Al was used in order to simultaneously obtain protons of 180 and 155 MeV energy. The detector prototype was positioned downstream the beam line behind a Double Sided Si Strip Detector, providing position data for the incoming proton beam. A flash ADC was used to digitize the entire pulse using a 1ns resolution for off-line analysis. The energy spectra obtained is shown in the figure. The spectrum is overlaid in red with the resulting energy spectra obtained from a GEANT4 simulation of the full set-up including beam tube, degrader and Si detector, an excellent agreement is obtained (Fig. 31).

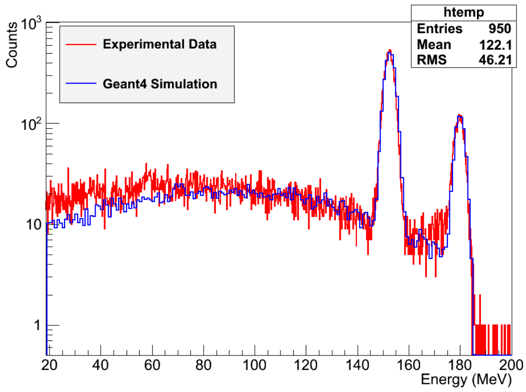

Fig. 31 Total energy in Phoswich, Comparison of exp. Data in red with Montecarlo simulation in blue

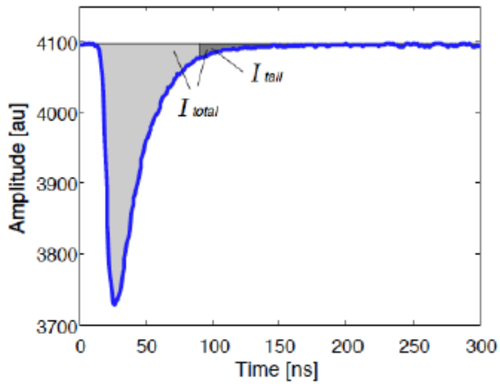

Fig. 32 The figure illustrate how is defined Tail vs Total Integration of the of pulse obtained from the Phoswich

As a flash ADC was used and the full pulse shape was recorded one can make an pulse shape analysis of the data (Fig. 32, 33). Comparing the full integral of the digitized pulse with that of the tail, as marked in the figure energy loss in the LaBr is attained. The extrapolated line beyond this point corresponds to larger energy loss in the LaBr due to reactions in the material. Notice that the higher energy breaks out earlier as an effect of the smaller energy-loss at higher energy. This work was published as; *"LaBr3(Ce):LaCl3(Ce) Phoswich with Pulse Shape Analysis for High Energy Gamma-ray and Proton Identification"* in [9] Nuclear Instruments & Methods A704 , 19-26, (2013) .

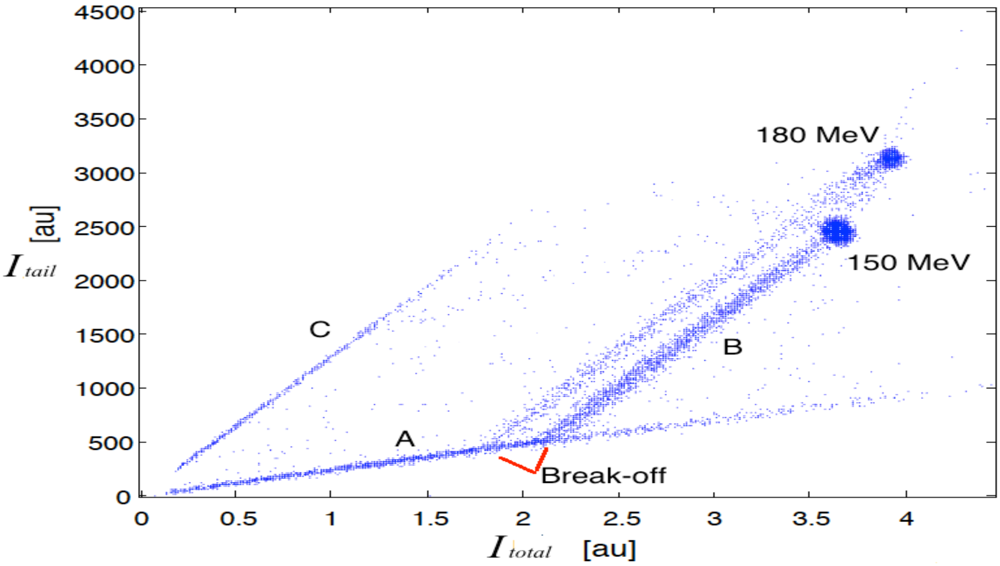

Fig. 33 The plot depicts I_{tail} vs I_{total} for the phoswich detector when irradiated with two discrete proton energies (180 and 150 MeV). Protons depositing the full energy in the phoswich combination, acting as a DE E telescope, correspond to the two main spots. The other patterns seen in the plot all correspond to protons depositing only parts of their energy due to scattering out of or into the active volume. Scattering out of the LaBr, leading to partial energy deposit in the first part, form the line A in the plot. With increasing energy deposition, the line bifurcates at a break-out point where the maximum energy loss in 1st crystal is obtained.

CEPA4 prototype: The R&D led to the construction of a prototype CEPA4 consisting in a 2x2 crystal cluster of 4 cm long $LaBr_3$(Ce) coupled with 6cm long $LaCl_3$(Ce) crystals in Phoswich configuration. Figure 34 illustrate the CEPA4 configuration when coupled to 4 HAMAMATSU R5380 8 stage PMtubes. The CEPA4 configuration was simulated using the GEANT4 package (see fig 35) and in March 2013 the response of CEPA4 to high energy protons (70 - 230 MeV in steps of 10 MeV) was tested using the cyclotron in Krakow. These data have been fully analysed and details can be found in the article "Proton response of CEPA4: A novel LaBr3(Ce)–LaCl3(Ce) phoswich array for high-energy gamma and proton spectroscopy" [25] Nuclear Instruments & Methods A769,105-111,(2015) and in the Technical Design Report of the forward part of the spectrometer CALIFA [26] .

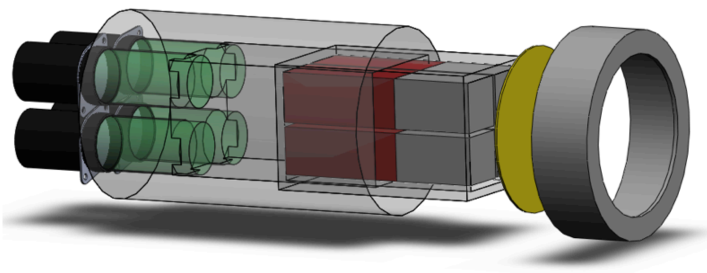
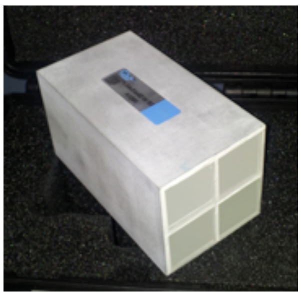

Fig. 34 Schematic illustration of CEP4 coupled to 4 R5380 8-stage PM-tubes. To the right a photograph of the scintillator package can be seen; including the 0.5 mm Al encapsulation ended with 4 optically isolated 5mm glass windows in order for the scintillator light to reach the readout sensors.

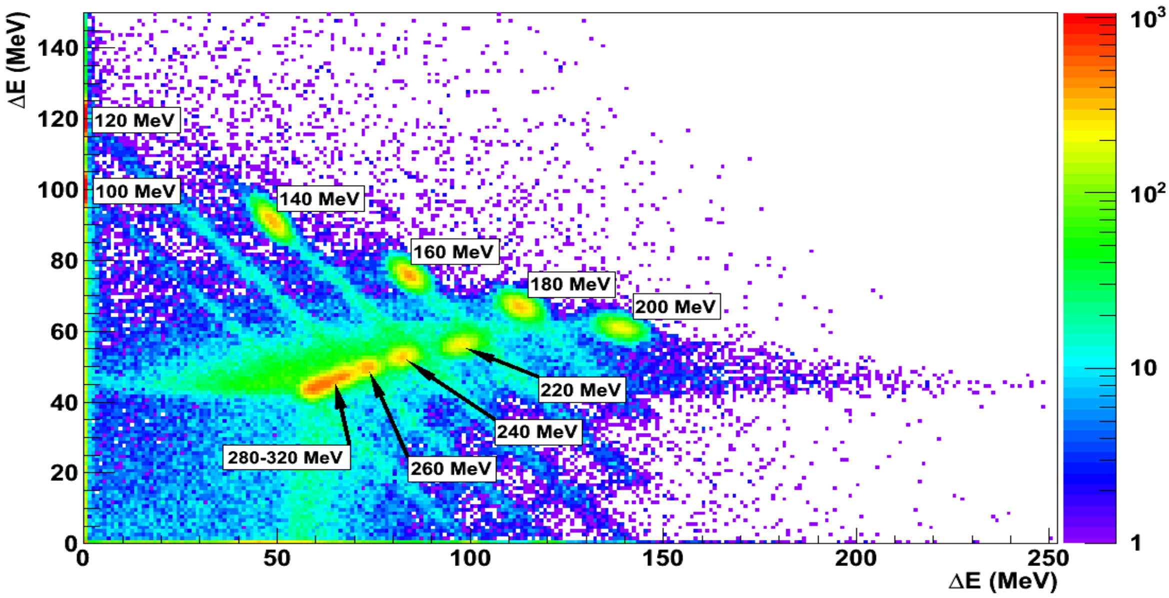

Fig. 35 The figure shows the two dimensional energy loss spectrum for protons between 100-320 MeV in steps of 20 MeV simulated with Geant4 for an Phoswich array with 4 cm $LaBr_3(Ce)$ and 6 cm $LaCl_3(Ce)$. Proton energy reconstruction with a resolution better than 5% is possible over the full energy range.

The Fig. 36 displays the actual data obtained in the experiment in Krakow; the energy deposited in the LaBr3 versus the total energy deposited in the phoswich unit. An add-back procedure has been used on an event-by-event basis so that we have added the energy deposited in all four crystals. However, we have carried out a multiplicity analysis (number of phoswich units fired per event) and have concluded that very few events do actually deposit energy in more than one phoswich unit, which happens only for the higher energies. In particular, for 90 MeV protons only 1.7% of the events have multiplicity higher than 1, for 150 MeV: 4.5%, and for 220 MeV: 21.2% (of which less than 1% have multiplicity 3).

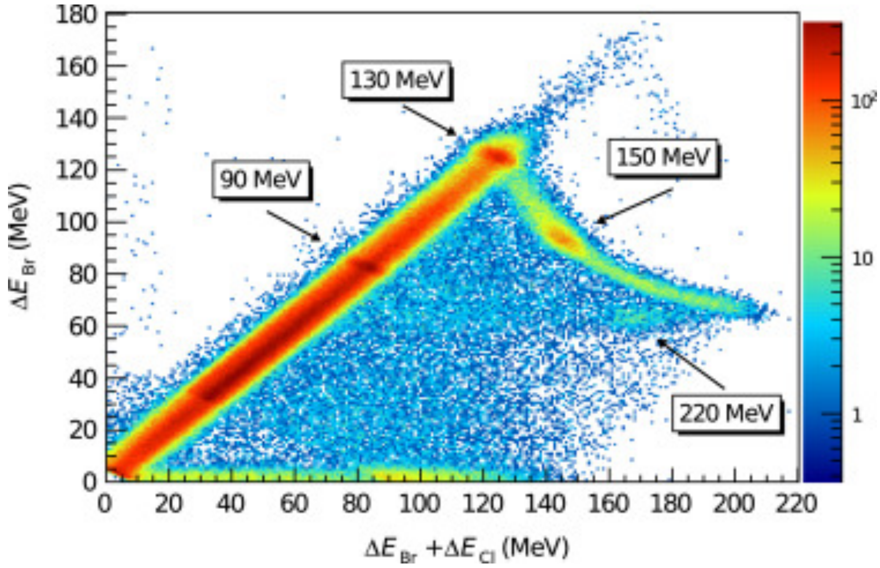

Fig. 36 Two-dimensional ΔE-E plot adding together different runs of mono-energetic proton energies: 90, 130, 150 and 220 MeV. The vertical axis represents the energy deposited in the LaBr3 crystal and the horizontal axis the total energy deposited in the Phoswich (ΔE+E).

In the plot of Fig. 36 we can clearly see the spot corresponding to 90 MeV protons, fully absorbed in the first crystal of the phoswich, namely the LaBr3. Continuing along the diagonal we find the spot of the 130 MeV protons. These are at the limit of absorption in the first crystal, all energies above will pass through the LaBr3 and enter the LaCl3 crystal. One of such examples are the 150 MeV protons that we can see as a spot in the banana corresponding to all the protons stopped in the second crystal. Finally, it is more difficult to visualize, but we have also included the spot which corresponds to the 220 MeV protons that pass through the entire length of the phoswich unit. We can zoom in Fig. 36 pointing at the 220 MeV spot and change to the three-dimensional representation as seen in Fig. 37. In this way we can have an impression of the ability of the CEPA4 detector combined with the pulse-shape analysis to separate the 220 MeV protons that have passed through the detector from the continuum at lower energies.

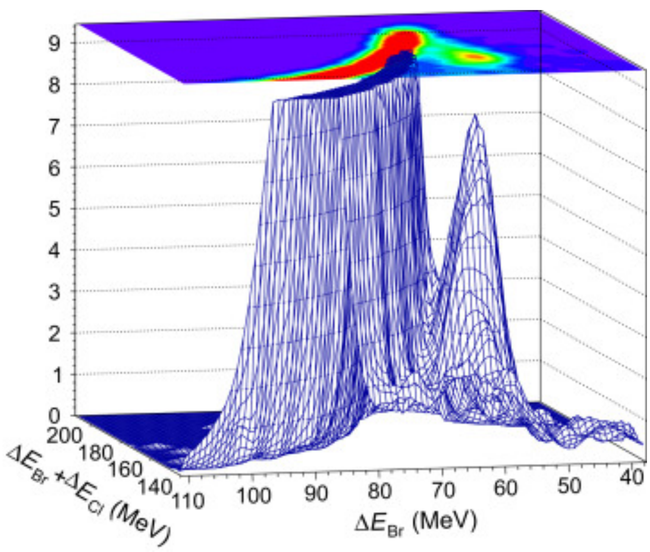

Fig. 37 Same as Fig. 39, but in a 3D-representation. The graph is zoomed around the spot at 220 MeV and a smoothing has been applied on the data.

This implies that, with the appropriate unfolding algorithm, one can reconstruct the original energy of the protons even at the energies that push the Bragg peak out of the volume of the detector. Furthermore, at 220 MeV we still separate the peak from the neighbouring energies with a resolution of around 7%.

To obtain an efficient readout system of the scintillators the IEM group is making R&D y characterization of different Digitizers: testing different Digital Pulse Processing & Pulse Shape Discrimination (DPP-PSD) firmware upload into the FPGA. One interesting way has been the design of a specifically Data Acquisition Software based on NI LabView to implement Digital Pulse Processing – Pulse Shape Discrimination (DPP-PSD) using the Caen V1742 ADC. This specifically designed software can calculate important parameters such as rise/fall time, peak, total energy and tail energy of the signals digitized by this ADC. Indeed, it could be possible to discriminate between different kinds of particles detected by the phoswich scintillator detector. By the use of different gamma sources (60Co / 22Na / 137Cs) and the CEPA4 prototype whose temporal signals has been digitized by the Caen DT5730 digitizer as well as with the V1742 ADC, it was possible to setup the software parameters to get energy histograms (calculating the peak energy resolution of the sources) and also pulse shape discrimination.

This detector, although conceived and built as a prototype for the final design of CEPA for CALIFA R3B, has its own applications in experiments investigating nuclear β -decay, and the reactions of low energy radioactive beam due to its high performance in spectroscopy of gamma rays and protons. We have optimized the readout using different sensors. Especially a very compact new metal-package photo-tube that resist high magnetic fields (<30mT).

Furthermore, we are exploring the use and applications of CEP4 to medical physics, in particular to perform high-accuracy dosimetry in hadron-therapy with ^{12}C beams as well as proton tomography.

References

[1] http://www.crystals.saint-gobain.com/BrilLanCe_380_Scintillator.aspx
[2] D.R. Schaart et al., Phys.Med.Biol. 54 (2009) 3501 and refs. cited
[3] A.Iltis et al. NIM A563(2006) 359
[4] M.Moszynski et al. NIM A567 (2006) 31
[5] M.Moszynski et al. NIM A568 (2006)739
[6] P.Menge et al. NIM A579(2007)6
[7] R. Nicolini et al NIM A 582 (2007) 554–561
[8] A.Giaz et al NIM A729(2013)910
[9] A. Maj et al ACTA PHYSICA POLONICA B40 (2009)565-575
[10] W.M. Higgins et al. J. Crys. Growth 310 (2008) 2085
[11] Degenhardt et al., IEEE NS Conf. Proc. 2009
[12] J.E. McFee et al.NIM-A712(2013)93-101
[13] A. Faust et al IEEE NSS_mic - conference record Pages: 2283-2291 (2009)
[14] B. Budden et al. NIM-A 652(2011)610
[15] R.Pani et al., NIM-A 787(2015)46
[16] R.Pani et al., JINST 10(2015) C06002
[17] V. G. Kiptily, et al. Plasma Phys. Control. Fusion 48 (2006) R59
[18] V.G.Kiptily et al. Rev. Sci. Instrum. 74 (2003) 1753.
[19] M. Tardocchi et al. Rev. Sci. Instrum. 79 (2008) 10E524.
[20]O.Wieland et al. IEEE-TNS 48(2001)296
[21] O.Wieland et al NIM A487(2002)441 and TNS 48(2000)
[22] F.C.L. Cespi et al NIM A570(2006)459
[23] H.J. Wollersheim NIM A 537(2005) 637
[24] S. Akkoyun et al. NIM A 668(2012)26
[25] F.C.L. Cespi et al NIM A593(2008)440
[26] J.W.Scrimger, R. G. Baker, Phys. Med. Biol. 12(1967)101
[27] A.Giaz et al. NIM A 772(2015)103-111
[28] P. Busca et al. 2011 IEEE NSS-MIC CONFERENCE Record pg. 419-422 and 2013
[29] F. Birocchi et al. 2010 IEEE NSS-MIC Conference Record Pages: 198-200 DOI: 10.1109/NSSMIC.2010.5873746
[30] L. Boschini,, C. Fiorini, IEEE. Nucl. Sci. Symposium 1 (1999) 464.
[31] N.Blasi et al to be submitted on NIM-A
[32] S.Brambilla, et al., 2012 IEEE NNS and MIC Conference Record, 1087.
[33] Scalable Silicon Photo-multiplier Array (Datasheet), SensL, http://sensl.com

GANAS Publication list

[1] Preliminary investigation of scintillator materials properties: SrI2:Eu, CeBr3 and GYGAG:Ce for gamma rays up to 9 MeV
Giaz, A.; Hull, G.; Fossati, V.; et al.
Nuclear Instruments & Methods A 804 (2015) 212-220

[2] Investigation on gamma-ray position sensitivity at 662 keV in a spectroscopic 3" x 3" LaBr3:Ce scintillator
Giaz, A.; Camera, F.; Birocchi, F.; et al.
Nuclear Instruments & Methods A 772 (2015) 103-111

[3] Position sensitivity in 3 " x3 " Spectroscopic LaBr3:Ce Crystals
Blasi, N.; Giaz, A.; Boiano, C.; et al.
Conference: Workshop on Applications of Novel Scintillators for Research and Industry (ANSRI) Book Series: Journal of Physics Conference Series Volume: 620 Article Number: 012004 Published: 2015

[4] Characterization of new scintillators: SrI2:Eu, CeBr3, GYGAG:Ce and CLYC:Ce
Giaz, A.; Fossati, V.; Hull, G.; et al.
Conference: Workshop on Applications of Novel Scintillators for Research and Industry (ANSRI) Book Series: Journal of Physics Conference Series Volume: 620 Article Number: 012003 Published: 2015

[5] Phototube non-linearity correction technique
Riboldi, S.; Blasi, N.; Brambilla, S.; et al.
Conference: Workshop on Applications of Novel Scintillators for Research and Industry (ANSRI) Book Series: Journal of Physics Conference Series Volume: 620 Article Number: 012007 Published: 2015

[6] New Scintillator Materials For Future And Present Facilities
Camera, Franco; Giaz, Agnese
Conference: Carpathian Summer School of Physics Location: Sinaia, ROMANIA Date: JUL 13-26, 2014 EXOTIC NUCLEI AND NUCLEAR/PARTICLE ASTROPHYSICS (V). FROM NUCLEI TO STARS Book Series: AIP Conference Proceedings Volume: 1645 Pages: 253-258 Published: 2015

[7] Development of a detector based on Silicon Drift Detectors for gamma-ray spectroscopy and imaging applications
Busca, P.; Butt, A. D.; Fiorini, C.; et al. Journal of Instrumentation Volume: 9 Article Number: C05005 Published: MAY 2014

[8] Characterization of Large Volume 3.5 " x 8 " LaBr3:Ce Detectors for the HECTOR+ array
Camera, F.; Giaz, A.; Pellegri, L.; et al. Edited by: Lunardi, S; Bizzeti, PG; Kabana, S; et al. International Nuclear Physics Conference (INPC) Firenze, ITALY JUN 02-07, 2013, INPC 2013 - VOL. 2 EPJ Web of Conferences Volume: 66 Article Number: 11008 Published: 2014

[9] Characterization of large volume 3.5 " x 8 " LaBr3:Ce detectors
Giaz, A.; Pellegri, L.; Riboldi, S.; et al.
Nuclear Instruments & Methods A 729 (2013) 910-921

[10] Performances of a 1"times1" Cs_2LiYCl_6 scintillator detector
Pellegri, L.; Bizzarri, E.; Blasi, N.; et al.
IEEE Nuclear Science Symposium and Medical Imaging Conference (2013 NSS/MIC) Seoul, South Korea, 27 Oct.-2 Nov. 2013

[11] Investigation of imaging and spectroscopy performances of a 1"times1" $LaBr_3$:Ce scintillator readout by Silicon Drift Detectors for nuclear physics measurements
Busca, P.; Butt, A.D.; Fiorini, C.; et al.
IEEE Nuclear Science Symposium and Medical Imaging Conference (2013 NSS/MIC) Seoul, South Korea, 27 Oct.-2 Nov. 2013

[12] Position sensitivity in a 3" times 3" $LaBr_3$:Ce scintillator Giaz, A.; Camera, F.; Blasi, N.; et al.
IEEE Nuclear Science Symposium and Medical Imaging Conference (2013 NSS/MIC) Seoul, South Korea, 27 Oct.-2 Nov. 2013

[13] Properties of a very large volume LaBr3:Ce detector
Giaz, A.; Pellegri, L.; Riboldi, S.; et al.
IEEE Nuclear Science Symposium / Medical Imaging Conference Record (NSS/MIC) / 19th Room-Temperature Semiconductor X-ray and Gamma-ray Detector Workshop Location: Anaheim, CA Date: OCT 29-NOV 03, 2012 Pages: 331-334

[14] Active Voltage Divider for Improved Estimation of Interacting Radiation Energy with Photomultiplier Tubes Coupled to High Light Yield Scintillators
Riboldi, Stefano; Camera, Franco; Blasi, Nives; et al.
IEEE Nuclear Science Symposium/Medical Imaging Conference (NSS/MIC)/18th International Workshop on Room-Temperature Semiconductor X-Ray and Gamma-Ray Detectors Location: Valencia, SPAIN Date: OCT 23-29, 2011, Pages: 776-778

[15] Recent developments in gamma-ray spectroscopy with new scintillators, LaBr3(Ce), to investigate nuclear structure at high excitation and far from stability
Pellegri, L.; Birocchi, F.; Bracco, A.; et al.
178th Course of the International School of Physics Enrico Fermi on From the Big Bang to the Nucleosynthesis Location: Varenna, ITALY Date: JUL 19-24, 2010.

[16] "Proton response of CEPA4: A novel LaBr3(Ce)–LaCl3(Ce) phoswich array for high-energy gamma and proton spectroscopy",
E. Nácher et.al. Nuclear Instruments & Methods A769,105-111,(2015),

[17] *"LaBr3(Ce):LaCl3(Ce) Phoswich with Pulse Shape Analysis for High Energy Gamma- ray and Proton Identication",*
O. Tengblad et.al. Nuclear Instruments & Methods A704 , 19-26, (2013) .

[18] CEPA: A LaBr3(Ce)/LaCl3(Ce) phoswich array for simultaneous detection of protons and gamma radiation emitted in reactions at relativistic energies
EPJ Web of Conferences 66, 11033 (2014)

[19] CALIFA, a Dedicated Calorimeter for the R3B/FAIR
Nuclear Data Sheets 120 (2014) 99–101
http://igfae.usc.es/~r3b/index.php?option=com_content&view=article&id=1&Itemid=2.

[20] CALIFA Barrel prototype detector characterisation
NIM A729 (2013) 77-84

[21] Test of PARIS LaBr+NaI module for High-Energy Gammas
Acta Physica Polonica B448 (2013) 651-656

[22] RPID — A new digital particle identification algorithm for CsI(Tl) scintillators
European Physical Journal A. (2013) 49:69

[MB15] M. Bendel et al., iPhos, a new technique for the CALIFA CsI(Tl) calorimeter, J. Phys.: Conf. Ser. 587 **(2015)** 012049

[RW13] R. Wirth et al., Particle identification using clustering algorithms, Nuc. Inst. and Meth. A 717 **(2013)** 77–82

[MB13] M. Bendel et al., RPID — A new digital particle identification algorithm for CsI(Tl) scintillators, Eur. Phys. J. A **(2013)** 49: 69

Thesis:

[MW16] M. Winkel, Komplexe Pulsformalgorithmen und Teilchenidentifikation zur Echtzeit-Implementierung in CALIFA, PhD thesis Technische Universität München **(2016)**

[MB14] M. Bendel, Entwicklung einer neuartigen Nachweismethode hochenergetischer Teilchen im CALIFA-Kalorimeter**,** PhD thesis Technische Universität München **(2014)**

[BH14] B. Heiss, Experimental Verification of the iPhos Energy Reconstruction Method for the CALIFA Calorimeter, Master thesis Technische Universität München **(2014)**

[FL14] F. Löffler, Bestimmung der Raumladungszone einer APD mit Hilfe von Alphateilchen, Bachelor thesis Technische Universität München **(2014)**

[CP13] Ch. Pfeffer, Neuartige Phoswich Szintillationsdetektoren zum Teilchennachweis, Bachelor thesis Technische Universität München **(2013)**

[TS12] Thomas Stettner, Messaufbau zur Charakterisierung von Silizium-Avalanche-Photodioden für das CALIFA-Kalorimeter, Bachelor thesis, Technische Universität München, **(2012)**